

UISCEmod: Open-source software for modelling water level time series in ephemeral karstic wetlands

Joan Campanyà ^{a,*}, Ted McCormack ^b, Laurence William Gill ^c, Paul Meredith Johnston ^c, Andrea Licciardi ^d, Owen Naughton ^a

^a Department of the Built Environment, South East Technological University, Carlow, Ireland

^b Geological Survey Ireland, Booterstown Avenue, Booterstown, Blackrock, Ireland

^c Department of Civil, Structural and Environmental Engineering, Trinity College Dublin, Dublin, Ireland

^d Université Côte d'Azur, IRD, CNRS, Observatoire de la Côte d'Azur, Géoazur, Sophia Antipolis, France

ARTICLE INFO

Handling Editor: Daniel P Ames

Keywords:

Hydrology
Modelling
Groundwater
Wetlands
Karst
Bayesian

ABSTRACT

Characterizing ephemeral karstic wetlands through hydrological modelling is key for sustainable protection of their ecosystems and to understand and mitigate the impact of flooding events. UISCEmod is a new open-source software for modelling water level time series, focused on ephemeral karstic wetlands, that requires minimal input information. UISCEmod contains both experimental and lumped hydrological models, and the calibration process is automated following a Bayesian approach. The main outputs of UISCEmod include volume, stage, inflow and outflow model time series, calibrated model parameters, and the associated uncertainties. UISCEmod was evaluated at 16 representative sites in Ireland obtaining Nash-Sutcliffe Efficiency (NSE) and Kling-Gupta Efficiency (KGE) above 0.85 for both stage and volume time series for most of the sites, showing its potential for covering the need for a simple, pragmatic, and flexible framework for modelling water levels in ephemeral karstic wetlands with relatively limited input data requirements.

1. Introduction

Society is fundamentally dependent on the availability of ecosystem services for human well-being, health, and livelihoods (Costanza et al., 2014; Millennium Ecosystem Assessment, 2005; TEEB, 2010). In this context, wetlands are amongst the most valuable ecosystems on earth (Mitsch et al., 2015). They provide a broad range of ecosystem services such as carbon sequestration, water supply and purification, as well as providing habitats for wetland endemic and dependent species. However, biodiversity loss and climate change severely threaten wetland ecosystem integrity and represent two of the most urgent environmental challenges facing humanity in the coming decades (Mittermeier et al., 2011; Shin et al., 2022; Vörösmarty et al., 2010). Anthropogenic activities have significantly altered wetlands across the globe, with over 85% of wetland area estimated to have been lost over the past 50 years and much of the remaining wetlands significantly degraded (IPBES, 2019; Zedler and Kercher, 2005).

Wetlands can vary greatly in extent over seasonal timescales (Davidson et al., 2018). Temporary or ephemeral wetlands, that is

wetlands where surface water largely disappears annually or with an undefined pattern, perform a range of biological, biogeochemical and hydrological functions within the landscape (Allen et al., 2020; Calhoun et al., 2017; Zedler, 2003). The cyclical drying and rewetting plays an important role in enhancing biodiversity and provides a habitat for many protected flora and fauna. Examples of temporary wetlands are found across the globe in a variety of landscape settings, such as poljes of the Dinaric karst (Mayaud et al., 2019), Mediterranean vernal pools (Zacharias and Zamparas, 2010; Zedler, 2003), and prairie potholes (Johnson and Poiani, 2016; Seabloom and van der Valk, 2003).

A particular type of wetlands are ephemeral karstic wetlands that forms in topographic depression of karst limestone, such turloughs and polje lakes (Bonacci, 2013; Coxon, 1987; Cvijic, 1893; Drew, 2018). They tend to fill during the wet season and vanish during the dry season, with the floods lasting for weeks to months. These periodic flooding makes them unique in terms of ecology (Irvine et al., 2018) and a potential flood hazard to society during both exceptional and prolonged recharge (Gutiérrez et al., 2014; Naughton et al., 2017). Understanding and characterizing ephemeral karstic wetlands through hydrological

* Corresponding author.

E-mail address: Joan.Campanya@setu.ie (J. Campanyà).

models is key for a sustainable protection of these unique ecosystems, to mitigate the impact of flooding events on society, and to estimate and quantify their adaptation to climate change and its impacts on ecology, flooding, and water resources.

Hydrological models are inevitably a simplification of real hydrological processes that aid in understanding, predicting, and managing water resources. Based on a representation of the relevant physical processes, hydrological models for karst systems can be classified as: 1) empirical, or “black box”, when it is derived from experimentation or correlations between measured hydrologic outputs and inputs, 2) lumped when it conceptualize the physical processes at the scale of the whole system without modeling spatial variability explicitly, and 3) distributed when it discretize the system in two- or three-dimensional grids and require the assignment of characteristic hydraulic parameters and system states to each grid cell (Hartmann et al., 2014). Empirical models are data based and involve mathematical equations derived from input and output time series instead of from the physical processes of the catchment. The main advantage of empirical models is that they need little consideration of the hydrological features and processes of the system, which means that can be easily implemented and applied to large-scale studies with relatively small effort. However, these types of models do not provide in depth information about the system and because they are restricted to the limits of the data used to create them extrapolation is prone to increasing uncertainty. Some examples of empirical models include transfer functions (Ascott et al., 2017; Beven, 2012; Collenteur et al., 2019; Dreiss, 1982; Jakeman et al., 1990; Jukić and Denić-Jukić, 2006; Taylor et al., 2007) and machine learning (i.e. Basu et al., 2022; Beaudeau et al., 2001; Hu et al., 2008; Kurtulus and Razack, 2007). Lumped models based on water balance equations typically simplify the hydrological system to a set of storages and may include semi-empirical equations with a physical basis representing the behaviour of the storage components (Hartmann et al., 2012, 2013; Mackay et al., 2014; Mazzilli et al., 2019; Mudarra et al., 2019). These models do not require detailed information about the hydraulics of the aquifer system and provide more in-depth information about some key elements of the hydrological system in comparison to the empirical model. Although calibration is usually more complicated than for the empirical models, it is usually just based on input (rainfall/allogenic flows) and output (spring flows or flood volume) time series. Finally, distributed models consider state variables that are measurable and that are function of both time and space, and they require much higher level of input information, with hydraulic parameters, system states, and boundary conditions defined for each grid cell (Duran and Gill, 2021; Hartmann et al., 2014).

In the particular case of groundwater dependent wetlands in karst systems the location and size of conduits or fissures are usually unknown, which hinders the use of distributed hydrological models in these types of environment (Borghi et al., 2016). Although complex lumped hydrological models have been successfully applied to specific ephemeral karstic wetlands (Gill et al., 2013, 2021; Morrissey et al., 2020; Schuler et al., 2020), there is the need for a simple, pragmatic and flexible framework that can be applied to large scale studies.

In this paper the UISCEmod software for modelling and characterizing ephemeral karstic wetlands is presented. UISCEmod includes two hydrological models, empirical and lumped, that requires minimal input information (meteorological, water levels, and digital terrain models (DTM) data) to calibrate the models and to generate water level time series. The calibration process for both modelling approaches is automated following a Bayesian approach. The software was implemented with synthetically generated water level time series to verify the correct implementation of the calibration process, and its potential was evaluated with measured time series in ephemeral karstic wetlands from Ireland.

2. Study area

The study area is mostly located on the western limestone lowlands in the Republic of Ireland, hereafter referred to as Ireland (Fig. 1). Lying on the western seaboard of Ireland the area experiences a temperate Atlantic climate with a mean annual rainfall of approximately 1000 mm (Table 1). Seasonal changes in rainfall are gradual, with monthly averages typically at their lowest in April (60–80 mm), rising to a peak in around December or January (110–150 mm). Natural drainage in the region is largely dominated by groundwater flow. Karstification of the limestone bedrock is widespread and so groundwater flow is characterised by high spatial heterogeneity, low storage, and extensive interactions between groundwater and surface water (Naughton et al., 2018). During periods of excess rainfall, storage within the karst groundwater system rapidly reaches capacity, resulting in the flooding of topographic depressions at the surface. This typically occurs each winter, with the floodwaters draining back into the karst system during the drier spring and summer months (Fig. 2). This recurrent flooding has led to the widespread formation of ephemeral karstic wetlands (turloughs). There are over 400 recorded examples of turloughs across Ireland, with individual sizes varying from less than 1 ha to over 840 ha and with the total habitat area within Ireland estimated at between 56.8 and 63.4 km² (NPWS, 2019). The majority of turloughs are in the lowlands, between 0 and 100 m AOD, with the largest volumes of water, ~5e7 m³, observed at Coole Lough (Fig. 1 ID:6). The chosen study sites comprise 16 such wetlands (Table 1). Eight sites were monitored over the period 2006 to 2009 (Naughton et al., 2012), and all sites were monitored over the period 2016 to 2022 (McCormack et al., 2020).

The conceptual operation of these wetlands can broadly be described using two conceptual models; through-flow systems and surcharged-tank systems (Naughton et al., 2012). In the through-flow model the turlough basin effectively acts as a large sink, collecting recharge from the surrounding vadose zone, shallow groundwater systems and/or point recharge before it is discharged to the underlying karst groundwater system. In a surcharged-tank model the turlough acts as an overflow storage for an underlying conduit network, alternating between filling and emptying depending on the relative pressure in the turlough and conduit network (Gill et al., 2013; Morrissey et al., 2020). Surface evaporation is generally insignificant to the water budget of these wetlands due to the temperate seasonality of turlough flooding, typically occurring during the winter months. Direct precipitation and runoff can be significant, particularly in shallow, flat basins, but under flood conditions groundwater flow is the dominant hydrological process (Naughton et al., 2017).

Turloughs contain a range of wetland species of national and international importance (Sheehy Skeffington et al., 2006; Waldren, 2015), and are classified as a Priority Habitat in Annex 1 of the EU Habitats Directive (92/43/EEC) and as Groundwater Dependent Terrestrial Ecosystems (GWDTEs) under the Water Framework Directive (WFD, Directive 2000/60/EC). The distribution and composition of vegetation communities within individual wetlands is driven by the flood regime (e.g. depth, duration, frequency and timing of flooding) and, if the natural frequency-duration of the flooding is modified, impacts on the distribution of vegetation communities are likely (Bhatnagar et al., 2021). Under normal winter rainfall conditions, turlough flooding does not pose a significant flood hazard. However, during either extreme or prolonged rainfall events, water levels can exceed their normal bounds and cause widespread damage and disruption to the surrounding areas (Naughton et al., 2017).

3. Methods

3.1. Software design

UISCEmod was developed using the high-level and object-oriented Python programming language, v3.8. It includes two modelling

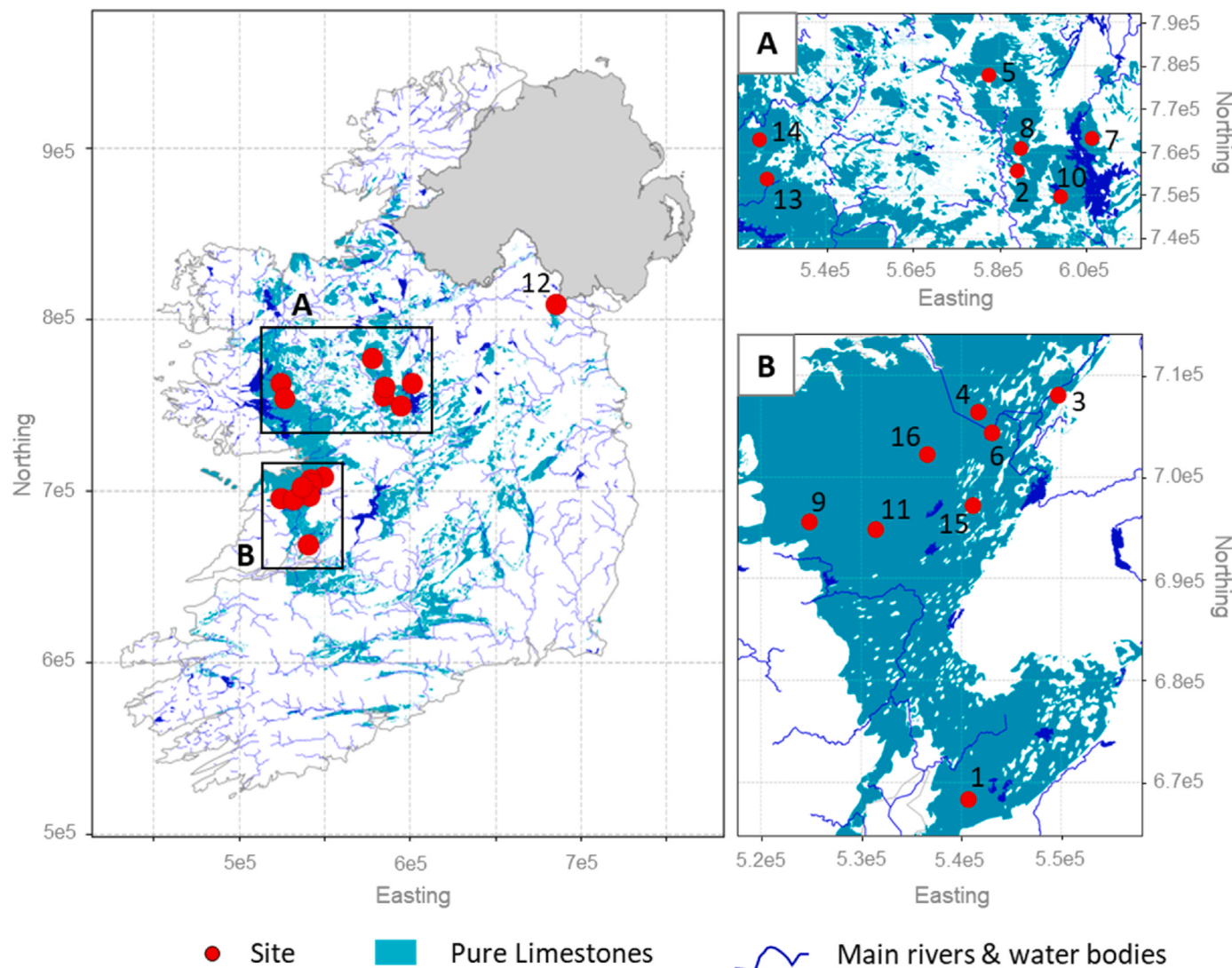


Fig. 1. Location of Ephemeral Karstic wetlands considered in this study (red dots). The cyan areas are related to regions with Carboniferous pure limestones. Blue lines show main rivers and water bodies from the environmental protection agency (EPA) database.

Table 1

Details about the sites considered in this study including name, coordinates, length of the time series used for calibration (CAL) and validation (VAL), maximum observed volume, area and stage, and long term annual average precipitation and evapotranspiration (ET).

ID	Site Name	Lat [deg.]	Lon [deg.]	Length [days] Cal Val	Max. Vol [m³]	Max. Stage [mOD]	Max. Area [m²]	Avg. Annual Precip. [mm]	Avg. Annual ET [mm]
1	Ballycar Lough	52.7623	-8.8783	428 365	2.93e6	24.65	9.73e5	1120	566
2	Ballygalda Turlough	53.5971	-8.2250	1097 550	4.80e5	50.48	2.55e5	1131	491
3	Blackrock	53.1209	-8.7517	2558 847	1.43e7	29.07	2,89e6	1252	505
4	Caherglassaun	53.1045	-8.8710	1888 851	2.41e7	10.79	6.72e6	1259	505
5	Castleplunket	53.7499	-8.3391	1129 458	1.92e6	88.72	7.48e5	1177	491
6	Coole Lough	53.0862	-8.8498	1067 458	4.58e7	13.40	1.02e7	1252	505
7	Fortwilliam Turlough	53.6191	-7.9762	1042 608	8.89e5	44.36	4.80e5	1005	491
8	Lisduff	53.5513	-8.2381	1190 423	5.86e5	49.99	4.81e5	1082	491
9	Lough Aleenaun	53.0055	-9.1203	1888 846	6.77e6	76.46	1.02e6	1636	505
10	Lough Funshinagh	53.4981	-8.0849	1097 366	1.86e7	69.03	5.43e6	1059	491
11	Lough Gealain	52.9995	-9.0212	987 538	1.03e6	30.98	3.76e5	1472	505
12	Moylan Lough	54.0219	-6.6699	550 305	1.64e6	66.52	2.24e5	949	473
13	Shrule Turlough	53.5286	-9.1107	1248 397	3.16e6	28.31	1.95e6	1234	490
14	Skealoghan	53.6112	-9.1375	1676 1092	2.00e6	34.14	1.85e6	1249	490
15	Termon South	53.0219	-8.8767	1827 821	1.06e6	23.42	4.72e5	1239	505
16	Tulla Turlough	53.0670	-8.9457	904 262	4.37e6	15.94	1.58e6	1466	505

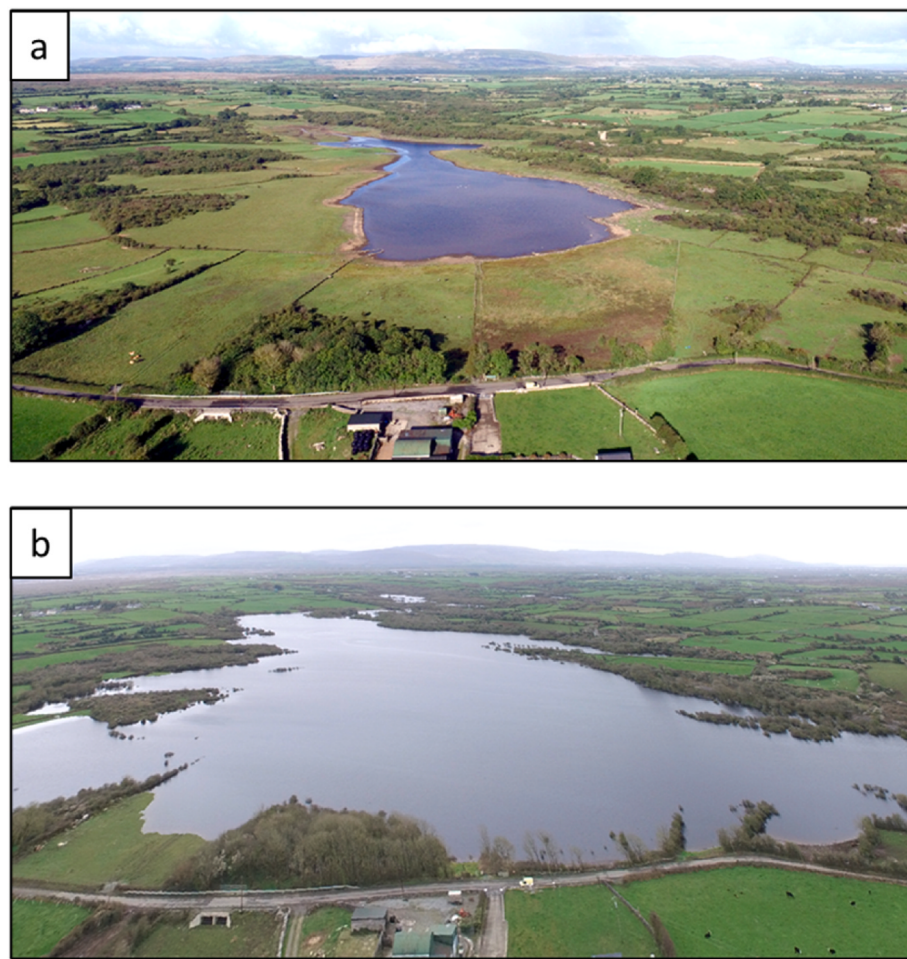


Fig. 2. Aerial images of Caherglassaun, Co. Galway, Ireland. a) August 2018 (dry season), b) March 2019 (end of wet season).

approaches, an experimental model (EM) based on a gamma distribution, and a lumped conceptual model (LM) based on a storage model. While both modelling approaches are a variant of the conceptual storage model (i.e. (Nash, 1960)), there are differences between them. The EM treats the system as a whole, providing information about the behaviour of the hydrological system but without providing direct information about the individual components of the system. In contrast, the LM approach distinguishes between inflow and outflow mechanisms, providing inflow and outflow model time series, considers the dependency of the outflow with the depth of the flood, accounts for direct interaction with the atmosphere (direct rainfall and evaporation), and has the potential to incorporate specific information about the site (e.g. elevation of potential outflow mechanisms) into the model parameters.

For both approaches, the modelling of water level time series is based on input meteorological data, rainfall (R) and reference evapotranspiration (ET_0), which are combined to generate effective rainfall (ER) time series using a soil moisture deficit model (Schulte et al., 2005). ER time series are then considered by the EM and LM models to generate first volume and then stage time series. In the case of the LM approach, inflows and outflows from direct interaction with the atmosphere are also considered, including inflows from direct precipitation and outflows from evaporation (Evap). A summary of the main steps is presented in Fig. 3. Modelling is performed with volume time series, instead of water level time series, to account for the stage-dependency of storage within the wetlands and to facilitate interpretation of the model parameters. Conversion from volume to stage time series, and vice-versa, is carried out using the stage-volume relationship for the specific site extracted from the Digital Terrain Models (DTM).

3.1.1. Experimental model (EM)

The EM model is a mathematical operator that relates two or more datasets, such as ER time series (input) and volume time series (output). In this case the EM approach is based the combination of linear store models, where ER is transformed into flood volume within the wetland by routing it through a series of linear storages or Nash reservoirs (Nash, 1960), with the relationship between the storage in each reservoir (S) and the outflow (Q) given by (eq. (1)):

$$S = kQ \quad \text{eq. 1}$$

where k is a time constant or mean residence time for the reservoir (Nash, 1959; Shaw, 1994). When n linear reservoirs are combined in series, the unit hydrograph, $f(t)$, is of the form of a gamma function (eq. (2)).

$$f(t) = \left(\frac{t}{k}\right)^{n-1} \frac{e^{-t/k}}{k(n-1)!} \quad \text{eq. 2}$$

Mathematically the value of n does not have to be an integer but can be fractional. Then the k, n parameters represent an equivalent system as if all connected reservoirs had the same mean residence time. This approach was considered because of its simplicity and flexibility capable of providing a wide range of unit hydrograph shapes that have been proved useful for modelling groundwater floods (Ascott et al., 2017) and because it requires a small number of model parameters to calibrate. A more generalized approach for higher order transfer function models, combining multiple reservoirs in series or parallel, is presented in Beven (2012).

Under the EM approach, computation of the volume time series was

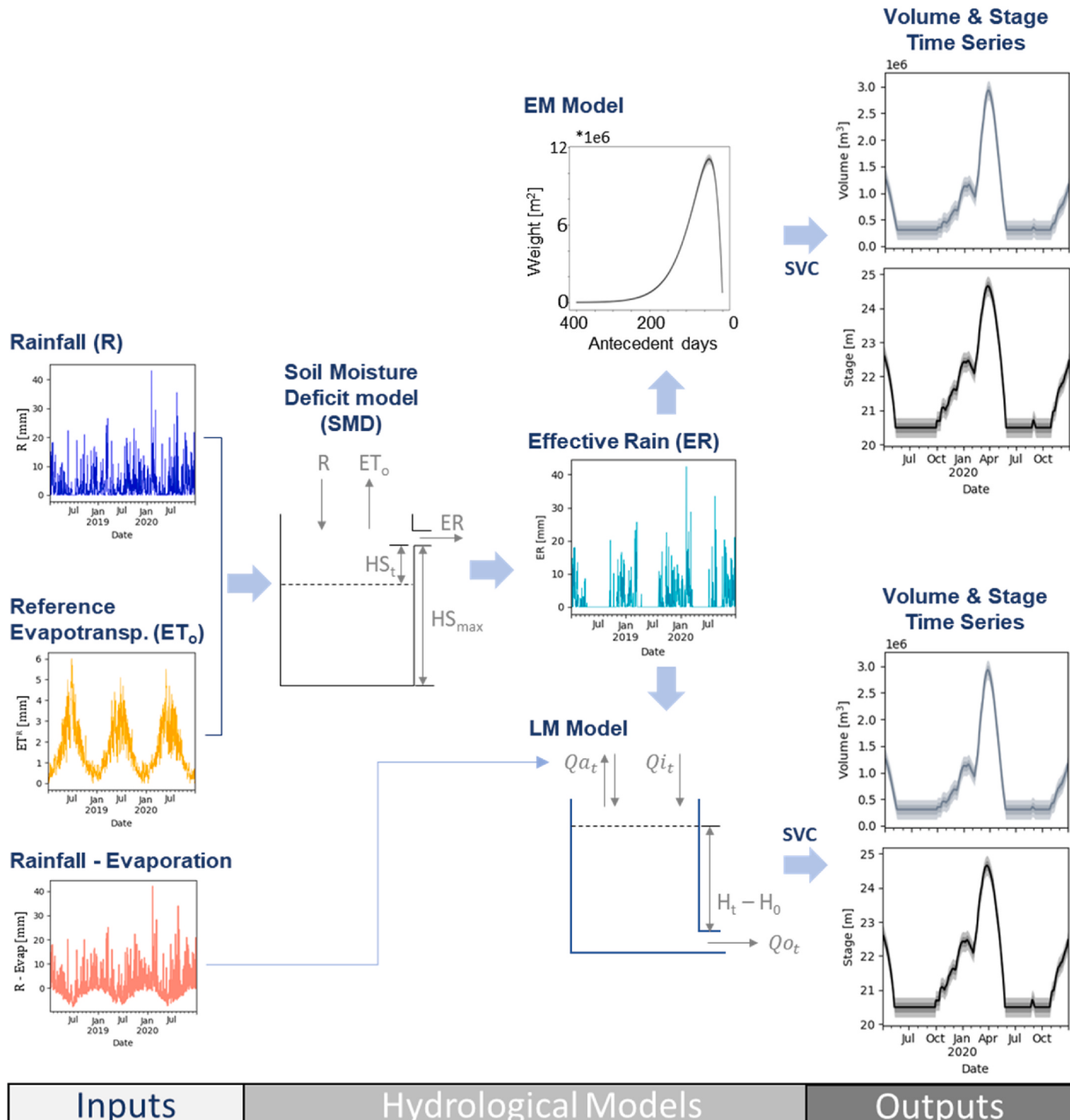


Fig. 3. Conceptual Diagram of UISCEmod.R: Rainfall, ET_o: Evapotranspiration, SMD: Soil Moisture Deficit Model, HS:Elevation to outflow for SMD, ER: Effective rainfall, Q_i:Inflow,Q_a: Inflow and outflow by direct interaction with atmosphere, H₀: Elevation of the outflow,Q_o:outflow., SVC: stage-volume conversion, EM: experimental model,LM: lump conceptual model.

performed following eq. (3):

$$V = C_0^{EM} + C_1^{EM} (f(t) * ER) \quad \text{eq. 3}$$

where V is volume time series, C_0^{EM} and C_1^{EM} are constants, with the super index EM to relate them with the EM modelling approach, and f is the transfer function (eq. (2)) that convolves over the ER time series. Based on this approach, four parameters (C_0^{EM} , C_1^{EM} , n , and k) need to be constrained to define the model.

3.1.2. Lumped model (LM)

The LM modelling approach is based on reservoir modelling, which considers the wetland site to act as a single reservoir, with distinct mechanisms controlling inflow and outflow to the reservoir separately. The inflow module combines ER and a flood routing reservoir to transform rainfall into an inflow signal at each time t , Q_i_t . The outflow module uses a characteristic set of discharge equations, based upon the water depth within the wetland, to generate an outflow value at each time t , Q_o_t . In this study, the outflow represents infiltration or drainage

from the wetland to the groundwater system. Direct interaction with atmosphere is represented by Qa_t including increase in volume due to direct rainfall and decrease in volume due to direct evaporation. The volume within the wetland at time t , V_t , is then calculated using water balance (eq. (4)):

$$V_t = V_{t-1} + Q_i_t - Qo_t + Qa_t \quad \text{eq. 4}$$

Looking at the inflow mechanisms, Q_i_t is based on ER and uses the gamma function (eq. (2)) to account for temporal changes in recharge entering the wetland per unit ER . The inflow is modelled following (eq. (5)).

$$Q_i_t = (C_1^{LM} - A) \bullet (f(t) * ER) \quad \text{eq. 5}$$

where C_1^{LM} is a constant value, with the super index LM relating it to the reservoir modelling approach. A is the area of the flood and is computed using volume-area curve extracted from the DTM.

The reservoir outflow, Qo_t , was calculated following (eq. (6)).

$$Qo_t = Qo^0 + Qo^1 \bullet (H_t - Ho)^\beta \quad \text{eq. 6}$$

where Qo^0 represents a constant flow and Qo^1 is the coefficient for the variable outflow. Qo^0 and Qo^1 are only considered if water level is above the elevation of the discharge point to the underground (Ho). H_t is the stage of the flood at time t , and β represents orifice coefficient for discharge.

Direct interaction with atmosphere was calculated following (eq. (7)).

$$Qa_t = A \bullet (R_t - Evap_t) \quad \text{eq. 7}$$

where R_t is the cumulative rainfall between t and $t-1$ and $Evap_t$ is the cumulative evaporation between t and $t-1$.

In summary, the LM approach requires the calibration of seven parameters ($C_1^{LM}, k, n, Qo^0, Qo^1, \beta, Ho$) to define the hydrological system, though Ho may be provided from DTM information, which would reduce the calibration to 6 parameters. In the case of $\beta = 1$, if Ho is not provided from external data, for any potential value of Ho , Ho' , a new value of Qo^0, Qo^0' , can be found that provides equivalent Qo_t , independently of the value of H_t and without affecting the other model parameters (eq. (8)). This means that in this case the calibration of these two parameters will not converge and only highlight the linear relationship between them. Because Ho is generally available from DTM and because it can complicate the calibration process, especially when $\beta \approx 1$, we recommend constraining Ho prior to inversion.

$$Qo^0' = Qo^0 + Qo^1 \bullet (Ho' - Ho) \quad \text{eq. 8}$$

3.1.3. Implementation

UISCEmod is divided in three modules: Inputs, Calibration, and Outputs (Fig. 4). The Inputs module combines meteorological datasets, R and ET_o , to generate ER time series, which are then considered for the hydrological models. The calibration module is used to calibrate the hydrological models and can be ignored if model parameters are already defined. The third module, Outputs, generates the products including: forward solution for stage and volume time series, probability density function (pdf) of the calibrated model parameters, and a set of products to help evaluating convergence of the calibration process as well as the fit of the data.

3.1.3.1. Inputs. The input module uses three main datasets: 1) continuous meteorological time series at daily steps with no missing data, including R , ET_o and $Evap_t$ time series, 2) water level time series at daily steps, in which missing data is allowed and considered as Nan , and 3) stage-volume conversion curves.

Within this module meteorological data is converted to ER using a

soil moisture deficit (SMD) model based on Schulte et al. (2005). The SMD model simplifies the system as a reservoir, which water level deficit at time t (Hs_t) is calculated by a mass balance for each time step (eq. 9) assuming that actual evapotranspiration, ET_A , decreases linearly to zero as Hs_t approaches a maximum deficit Hs_{max} (eq. 10). All variables are water depths in mm.

$$Hs_t = Hs_{t-1} - R_t + ET_{At} - ER_t \quad \text{eq. 9}$$

$$ET_{At} = ET_o \frac{Hs_{max} - Hs_{t-1}}{Hs_{max}} \quad \text{eq. 10}$$

Hs_t values can range between 0, the reservoir is full, and Hs_{max} , the reservoir is empty, where Hs_{max} is estimated during the calibration process. Any amount of precipitation that would bring Hs_t to negative values, above the outflow elevation, are considered as ER . On the other hand, Hs_{max} limits the maximum SMD, thus preventing the reservoir from becoming excessively under-saturated. Low Hs_{max} values would encourage the model to predict low level flood events and an earlier onset of flooding as less rainfall is required to exceed the SMD reservoir capacity. If not specified, $Hs_{t=0}$ is considered as 0.

Finally, based on eq. (9) and eq. (10), ER is computed following eq. (11):

$$ER_t = \begin{cases} R_t - Hs_{t-1} - ET_{At} & \text{if } R_t - Hs_{t-1} - ET_{At} > 0 \\ 0 & \text{if } R_t - Hs_{t-1} - ET_{At} \leq 0 \end{cases} \quad \text{eq. 11}$$

Input stage time series are also converted to volume time series using stage-volume curves, and all the input time series are then divided into calibration and validation datasets with the aim of assessing the potential of the hydrological models based on the credibility of its outputs (Klemes, 1986).

3.1.3.2. Calibration. Calibration of the model parameters is automated following a Bayesian approach. The resulting ensemble of accepted models is distributed according to the (unknown) target posterior pdf , from which summary statistics and uncertainties on individual model parameters are obtained. Description of model parameters considered during calibration and the units adopted within UISCEmod are summarized in Table 2.

Following the Bayesian formulation (eq. (12)), with θ being the set of parameters and D the set of observations (i.e. volume time series), the posterior pdf of the model parameters, $p(\theta|D)$ can be obtained from the prior pdf of the model parameters $p(\theta)$, the observed data $p(D)$, and the likelihood $p(D|\theta)$:

$$p(\theta|D) = \frac{p(D|\theta) \bullet p(\theta)}{p(D)} \quad \text{eq. 12}$$

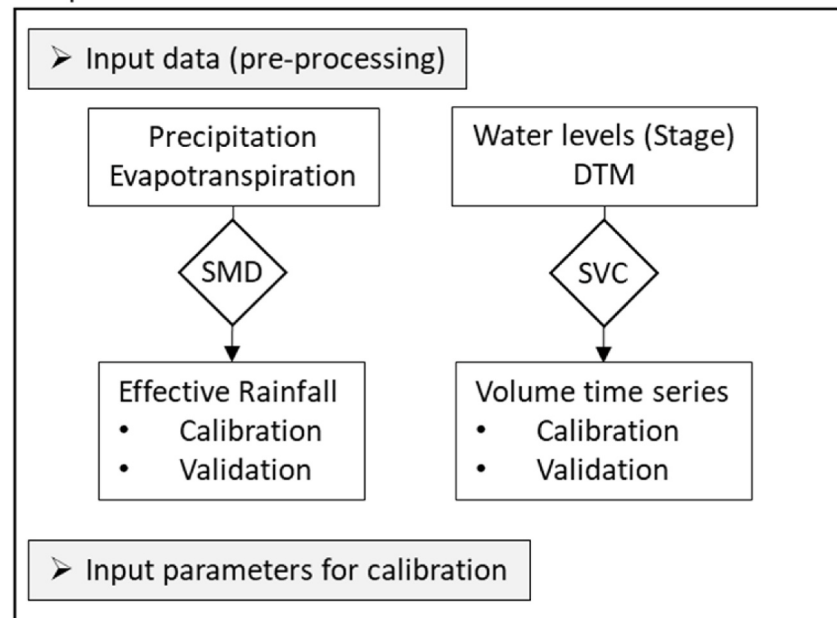
The unknown posterior distribution is sampled using the popular Metropolis Hasting algorithm (Hastings, 1970; Metropolis et al., 1953), a Markov chain Monte Carlo (McMC) implementation constituted by a two-step procedure. First, a candidate model (θ') is derived by perturbing the current model (θ) of the chain. Second, the candidate model is accepted with a probability α following the Metropolis rule (eq. (13))

$$\alpha = \min \left[1, \frac{q(\theta'|\theta) \bullet p(D|\theta') \bullet p(\theta)}{q(\theta|\theta') \bullet p(D|\theta') \bullet p(\theta')} \right] \quad \text{eq. 13}$$

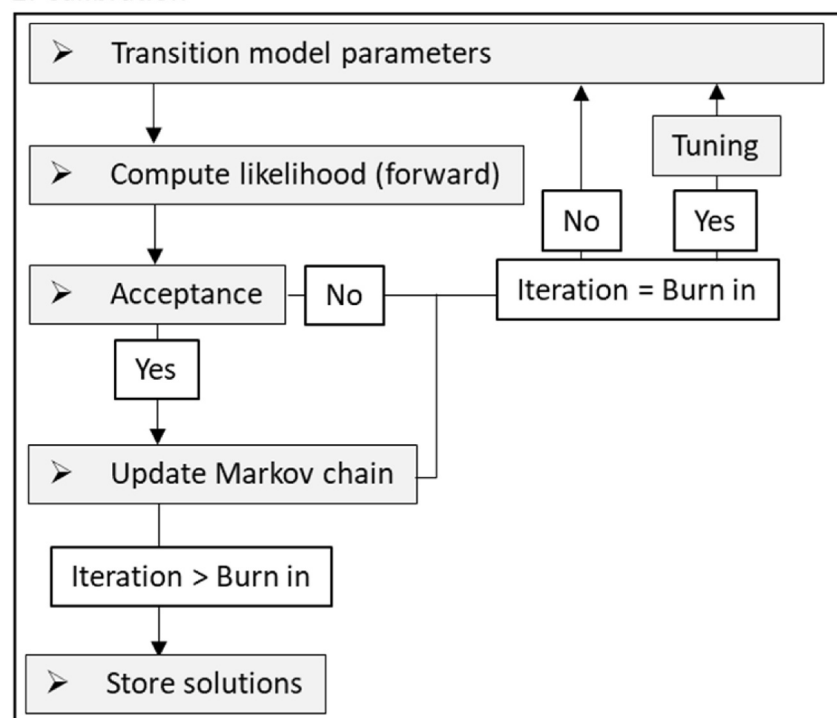
where $q(\theta'|\theta)$ is the proposal distribution, the probability of obtaining a candidate (θ') when the current model is (θ). Parts of the software related to the Metropolis Hasting McMC approach within calibration and evaluation modules were designed following recommendations from Hogg and Foreman-Mackey (2018).

If accepted, the candidate is stored and used as a current model in the next iteration of the chain, which means that each iteration of the McMC chain only depends on the current values of θ . In our particular case, where the data (D) is the same in each iteration and a priori none of the potential model parameters are more likely to explain the data, eq. (13)

1. Inputs



2. Calibration



3. Outputs

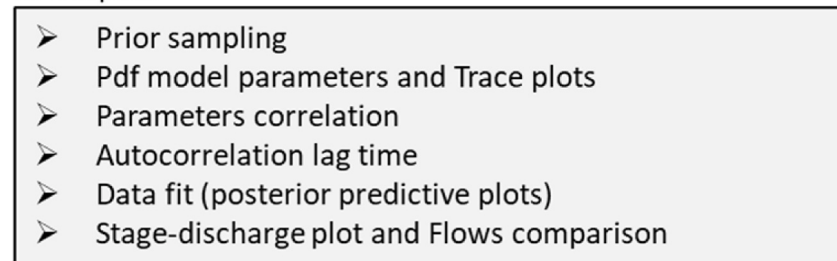


Fig. 4. UISCEmod Flowchart. gray boxes represent sub-modules, white boxes are related to conditions and steps within the sub-modules. SMD: Soil Moisture Deficit Model, SVC: stage volume conversion, DTM: Digital Terrain Model.

Table 2

Summary of model parameters to be considered during the calibration process. Parameters with * are recommended to be provided from external sources.

Hydrological Model	Parameter (units)	Description
Soil Moisture Deficit (SMD)	Hs_{max} (mm)	Maximum Soil Moisture Deficit
Experimental Model (EM)	C_0^{EM} (m^3)	Constant factor
	C_1^{EM} (m^2)	Scale factor
	n^{EM} (-)	Shape parameter gamma distribution
	K^{EM} (-)	Scale parameter gamma distribution
	σ^{EM} (m^3)	Uncertainties between measured and modelled time series assuming Gaussian distribution
Lump Model (LM)	C^{LM} (m^2)	Scale factor
	n^{LM} (-)	Shape parameter gamma distribution
	k^{LM} (-)	Scale parameter gamma distribution
	Qo^0 (m^3/day)	Constant outflow
	Qo^1 (m^2/day)	Coefficient for the variable outflow
	Ho (m)	Elevation of the wetland discharge point *
	β (-)	Orifice coefficient for wetland discharge
	σ^{LM} (m^3)	Uncertainties between measured and modelled time series assuming a Gaussian distribution

loses its dependency on $p(D)$, $p(\theta)$ and $p(\theta')$. In relation to the proposal distribution, the UISCEmod also imposes that $q(\theta|\theta')$ is the same as $q(\theta'|\theta)$. Following this approach, eq. (13) is simplified to only be dependent on the likelihood ratio between candidate and current models.

The transition between model parameters is carried out considering a simple version of the Gibbs sampling (Geman and Geman, 1984), perturbing only one parameter in each iteration. The initial step size is set to 1% of the range of possible values for each parameter. This approach was considered as it is easy to implement when the values of the model parameters differ by orders of magnitude.

In relation to the computation of the likelihood, UISCEmod assumes that the distance between the observed and modelled time series, the error residuals, are normally distributed around zero (eq. (14)).

$$p(D|\theta) = \frac{1}{\sqrt{2\pi\sigma^2}} e^{-\frac{(D-g(\theta))^2}{2\sigma^2}} \quad \text{eq. 14}$$

where $g(\theta)$ is the modelled time series and σ is the standard deviation on the data and is unknown. Note that because σ is not known a priori it can also be considered as a model parameter and estimated during the calibration process (Malinverno and Briggs, 2004).

During the calculation of the likelihood, only volumes of water above a defined threshold (i.e. above the data logger elevation) are considered. This discrimination is due to the nature of water level time series, as they may have flat sections when the dataloggers are dry. This implies that volumes of water beneath a certain threshold need to be replaced by the threshold value to fit the measured time series. This correction disagrees with the assumption that the error residuals around the true solution are normally distributed, as the corrected points would suggest a perfect fit, or a constant bias.

The calibration process proceeds iteratively and requires a number of burn-in iterations to converge to the posterior pdf. For this reason, models are saved for posterior inference only after the burn-in iterations are completed. Before inference, tuning is applied with the aim to speed up sampling of the pdf of the model parameters. During tuning, several step sizes are considered ranging between 0.0003% and 5% of the range of possible values for each parameter. Two criteria are applied when defining the optimal step size for each parameter, autocorrelation lag time and acceptance ratio. Autocorrelation lag time represents the number of steps required by McMC to produce an independent sample, i.e. the number of steps for autocorrelation to reduce to 0.2. The acceptance ratio is the ratio of accepted models in relation to the number of

iterations. The step size with lower autocorrelation lag time is considered as optimal. If multiple step sizes have equivalent autocorrelation lag time the step size with an acceptance ratio closest to the optimal acceptance ratio, based on Gelman et al. (1996), is chosen.

Finally, the uncertainties of the modelled time series are redefined following an empirical approach to account for epistemic uncertainty of the hydrological model, related to discrepancies caused by the lack of capacity of the hydrological models to adequately represent the governing physical processes. When working with measured data, it was observed that the constrained posterior data errors, σ , were significantly larger than the errors expected from the dataloggers (few millimetres), and that the measured time series were most of the time outside the 95% confidence interval from computing the forward solution using the accepted model parameters. This epistemic uncertainty of the hydrological models can be an issue when using UISCEmod as it can significantly underestimate the confidence intervals of the model time series. With the aim of providing model time series that include the measured water level time series within the confidence intervals, the quantiles 0.025, 0.16, 0.84 and 0.975 of the error residuals from the calibration process are considered to define 68% and 95% confidence intervals. The validity of this approach was evaluated during the validation process.

3.1.3.3. Outputs. The outputs module performs the forward calculations and assesses the confidence in the results by providing relevant information related to: 1) adequate sampling of the prior $p(\theta)$, 2) convergence of the calibration process and correlation between model parameters, 3) distribution of error residuals, and 4) data fit.

The sampling of the prior is used to corroborate that the sampling process follows the expected distribution of the prior, and it should be performed before starting the calibration process. This test is performed by running the calibration process setting the acceptance probability to 1 (i.e. all candidates are accepted). If the sampling process is well implemented, the pdf of the model parameters returned by the framework, $p(\theta|D)$, should be the same as the pdf of the prior $p(\theta)$.

Convergence of the calibration process can be evaluated by visualizing the $p(\theta|D)$, and by looking at the trace plots, which show the evolution of the accepted values associated with each parameter. These plots can indicate problems with both the hydrological model and the transition between model parameters, and qualitatively judge convergence when a smooth $p(\theta|D)$ is observed and the trace plots cross the median value multiple times. Corner plots, based on the predefined corner.py library (Foreman-Mackey, 2016), also help assessing convergence of the calibration process and highlight potential correlations between model parameters.

An additional output is the comparison between the distribution of the error residuals and the gaussian distribution of the accepted σ values. Error residuals following a normal distribution will bring confidence on the initial assumptions. Error residuals following a non-normal distribution may be an indication that certain parts of the data disagree with the initial assumptions, which may add a bias to the constrained model parameters and the confidence intervals.

Finally, the ability of the model parameters to reproduce the data is evaluated. Data fit is evaluated by considering Nash-Sutcliffe Efficiency (NSE) (Nash and Sutcliffe, 1970), Kling-Gupta Efficiency (KGE) (Gupta et al., 2009; Kling et al., 2012) parameters, and model bias (BIAS). BIAS is computed using normalized time series between 0 and 1 (min-max normalization), using the measured time series to define the normalization parameters, to facilitate comparison between sites and between volume and stage datasets. Following this approach, the BIAS is presented as a percentage of the amplitude of the signal (eq. (15))

$$BIAS = \frac{100}{n} \sum_{i=1}^n y'_i - \hat{y}_i \quad \text{eq. 15}$$

where y' and \hat{y} are normalized measured and modelled time series,

respectively, and n are the number of points within the time series.

The capacity at reproducing flood duration curves, showing the proportion of time that a certain volume is equalled or exceeded, is also considered due to its relevance on groundwater flood analysis (i.e., Morrissey et al., 2020; Naughton, 2011) and ecological studies of the wetlands (Bhatnagar et al., 2021; Casanova and Brock, 2000; De Becker et al., 1999).

3.2. Experimental design

Two experiments were designed to implement and to evaluate the potential of UISCEmod for modelling water level time series in ephemeral karstic systems. First, the implementation was focused on synthetically generated water level time series with the aim of corroborating the correct implementation of the calibration process. Second, the evaluation was performed with measured time series quantifying the accuracy of the framework at modelling water levels at 16 ephemeral karstic wetlands (Fig. 1). Details of the considered wetlands for the evaluation process are presented in Table 1.

Meteorological time series, rainfall (R), evaporation ($Evap$) and evapotranspiration (ET_o), for both implementation and evaluation processes were provided by the Irish Meteorological Service (Met Éireann). R data was extracted from a gridded dataset of 1×1 km resolution resulted from the interpolation of data from 500 meteorological stations, approx. (www.met.ie, Daily Rainfall and Temperature Grids). $Evap$ and ET_o time series from the nearest Met Éireann station with available data were considered for each site. Distance between the considered meteorological stations ranges between 45 and 75 km, with distance between the sites to the closest meteorological station ranging between 9 and 40 km. Water level time series were measured during two separate time periods. The first dataset includes 8 sites with continuous hourly measurement recorded between September 2006 and August 2009 using Schlumberger Diver™ pressure transducers and compensated for barometric pressure using a BaroDiver™ (Naughton et al., 2012). The second dataset includes data from all sites with hourly measurements recorded between November 2016 and January 2022 (McCormack et al., 2020). Water levels of the second dataset were monitored using Van Essen TD-Divers™ pressure transducer data loggers, and logger data were compensated with barometric data to yield water levels above the logger. In both cases vertical resolution of the dataloggers was less than 1 cm. Conversion from stage to volume was performed using stage-volume curves (SVC) created for each site from a national DTM for Ireland (McCormack et al., 2020), with horizontal resolution of 5×5 m and vertical resolution ranging between 0.1 m and 0.7 m. For all of the sites considered in this study the vertical resolution of the DTM was close to 0.1 m as Lidar datasets were used to improve the resolution of the national DTM in these regions (McCormack et al., 2020) and dGPS measurements were used to correct for potential regional vertical shifts of the DTM at each site.

The implementation process was carried out with two synthetic water level datasets, one for each modelling approach, to verify the correct performance of the calibration process. Synthetic water level

time series were generated using the parameters from Table 3, with values based on previous hydrological studies of karst systems in Ireland (i.e. McCormack et al., 2020; Naughton, 2011). Historic meteorological data, and stage-volume curve for Termon South (Co. Clare, ID:15) were considered to generate the synthetic water level time series. Gaussian noise was added to the synthetic time series to include uncertainties using the true σ parameter. Synthetic water level times series of four- and three-years duration were considered for calibration and validation, respectively.

Calibration and validation datasets for both implementation and evaluation process were defined based on the following criteria: 1) the calibration period should include the largest and smallest observed volumes, 2) a complete rising and recession phase must be included in both datasets, 3) the length of the calibration time series should be equal or longer than validation time series, and 4) if possible after considering points 1 to 3, the newest data should be considered for calibration and the oldest data for validation with the aim of calibrating the models with closest data to current hydrogeological conditions and with the most accurate datasets. Higher quality control standards were followed for the newest datasets, such as multiple dGPS measurements, with virtual reference station (VRS), along the flood seasons to corroborate the quality of the measurements. Based on these criteria, the percentage of time series used for calibration and validation was around 70%:30% for most of the sites, with minimum and maximum percentage of time series used for the calibration datasets being 54% and 76%, respectively. During this experiment the same sites and segments of the time series were considered for EM and LM modelling approaches to facilitate comparison between them.

4. Results

4.1. Implementation

The capacity of UISCEmod to converge on model parameters and accurately reproduce the synthetically generated water level series was first explored to validate the underlying modelling approach. Trace plots and histograms of the posterior pdf for each variable (Fig. 5) corroborated convergence of the calibration process and that the true parameters are within the posterior pdf. The capacity of the calibration process at recovering the data errors is presented in Fig. 6, comparing: 1) the distribution of the error residuals (blue), 2) the normal distributions generated with the accepted values for σ (black), and 3) the “true” errors added to the synthetic data (orange dashed line). In relation to data fit, NSE and KGE values above 0.98 were obtained for calibration and validation datasets for both modelling approaches, BIAS was centred at zero with interquartile range (IQR) being smaller than 1%, and the percentage of measured data points within the 68% and 95% confidence intervals was 68% and 95% for calibration and 70% and 94% for validation datasets for EM model, and 68% and 95% for calibration and 67% and 95% for validation datasets for LM model.

Table 3

True Model parameters for synthetic time series and the considered values during Implementation process.

EM	C_1^{EM}	C_0^{EM}	n^{EM}	k^{EM}	σ^{EM}	$H_{s,max}$		
True parameters	9.00e7	-1.05e5	2.04	10.4	9900	110		
Initial value	2.34e8	2500	3.5	37.5	7.0e4	90		
Range	min	0	-5e5	1	0.01	5		
	max	1.00e9	5e5	5	1e5	500		
LM	C_1^{LM}	n^{LM}	k^{LM}	Qo^1	Qo^0	β	σ^{LM}	$H_{s,max}$
True parameters	2.20e6	1.3	16.95	-2.12e3	-3.7e3	1.35	1.5e4	110
Initial value	1.21e5	4	1	-100	0	0.85	2.3e4	90
Range	min	0	0.01	-1e4	-1e4	0	1	5
	max	2.00e7	5	100	0	1e4	1e6	500

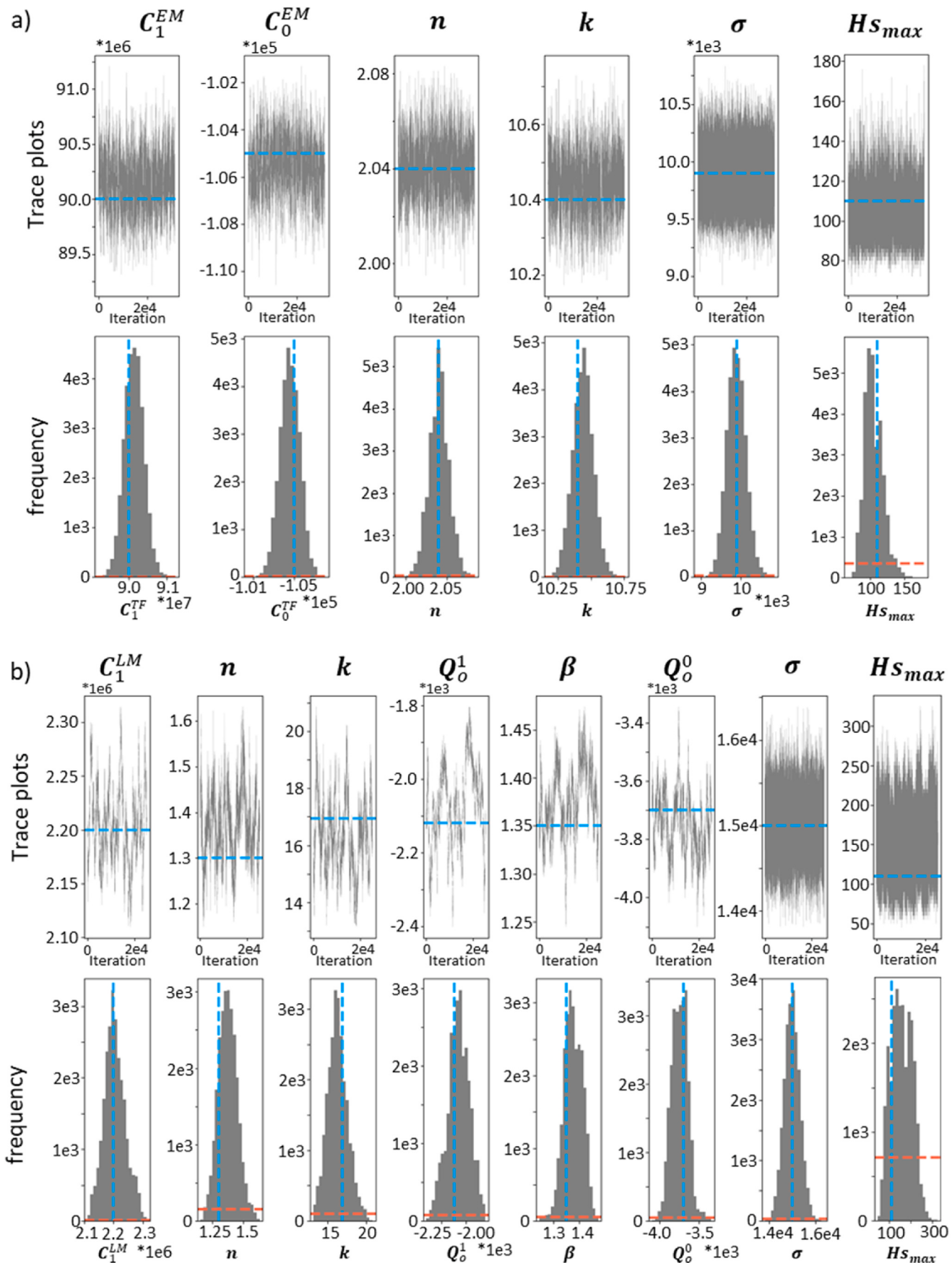


Fig. 5. Trace plots and histogram of the posterior pdf of the model parameters. a) EM model parameters, b) LM model parameters. Red horizontal line indicates distribution of the prior and the Blue lines reveal the true solution.

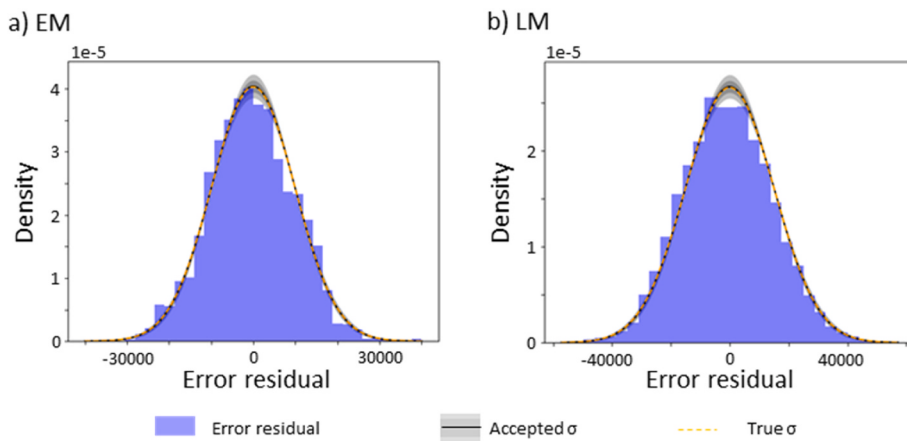


Fig. 6. Distribution of errors residuals (violet) compared to normal distribution centred at zero with standard deviation from constrained σ values (in black) and to normal distribution of the true errors (orange dashed line).

4.2. Evaluation

Performance metrics for the 16 sites used for the evaluation are presented in Table 4 and summarized in Fig. 7. Both modelling approaches were capable at modelling the water level time series with model performance NSE and KGE values above 0.85 for most sites for calibration and validation datasets, for volume and stage time series (Fig. 7a). In terms of BIAS, both calibration and validation datasets showed relatively small values for most of the sites, between -2% and 5% (Table 4). BIAS analysis for volume and stage time series for different flood levels (low ($[0.0, 0.25]$]), medium ($[0.25, 0.75]$) and high ($[0.75, 1.0]$)) is presented in Fig. 7b. Finally, to illustrate the performance of UISCEmod across the spectrum of recorded flood behaviours, three sites representative of the range of flood dynamics are shown in Fig. 8 for validation datasets.

The empirically defined confidence intervals were validated by looking at the percentage of measured data points within the defined confidence intervals for the modelled time series, for the validation dataset, with the results suggesting that the presented approach is reasonable. For the EM approach, most of the sites had between 60% and 77% of the points within the 68% confidence interval, and between 87% and 98% within the 95% confidence interval. For the LM approach most

of the sites had between 51% and 75% of the points within the 68% confidence interval, and between 80% and 99% for the 95% confidence interval.

In relation to computational time, based on computer with 31.7 GB of useable RAM with a processor of 11th Gen Intel® Core™ i7-1185G7 @3 GHz @1.80 GHz the EM was shown to be significantly faster than the LM approach. Each iteration within the calibration process for the EM approach took ~ 0.0025 s, which means that a calibration process considering 10^6 iterations can be performed in less than 1 h. For the LM approach, each iteration within the calibration process took ~ 0.1 s, which is over one order of magnitude slower than the EM approach, needing ~ 30 h for a calibration process of 10^6 iterations.

5. Discussion

5.1. Modelling water level time series in groundwater dependent wetlands

5.1.1. Data fit

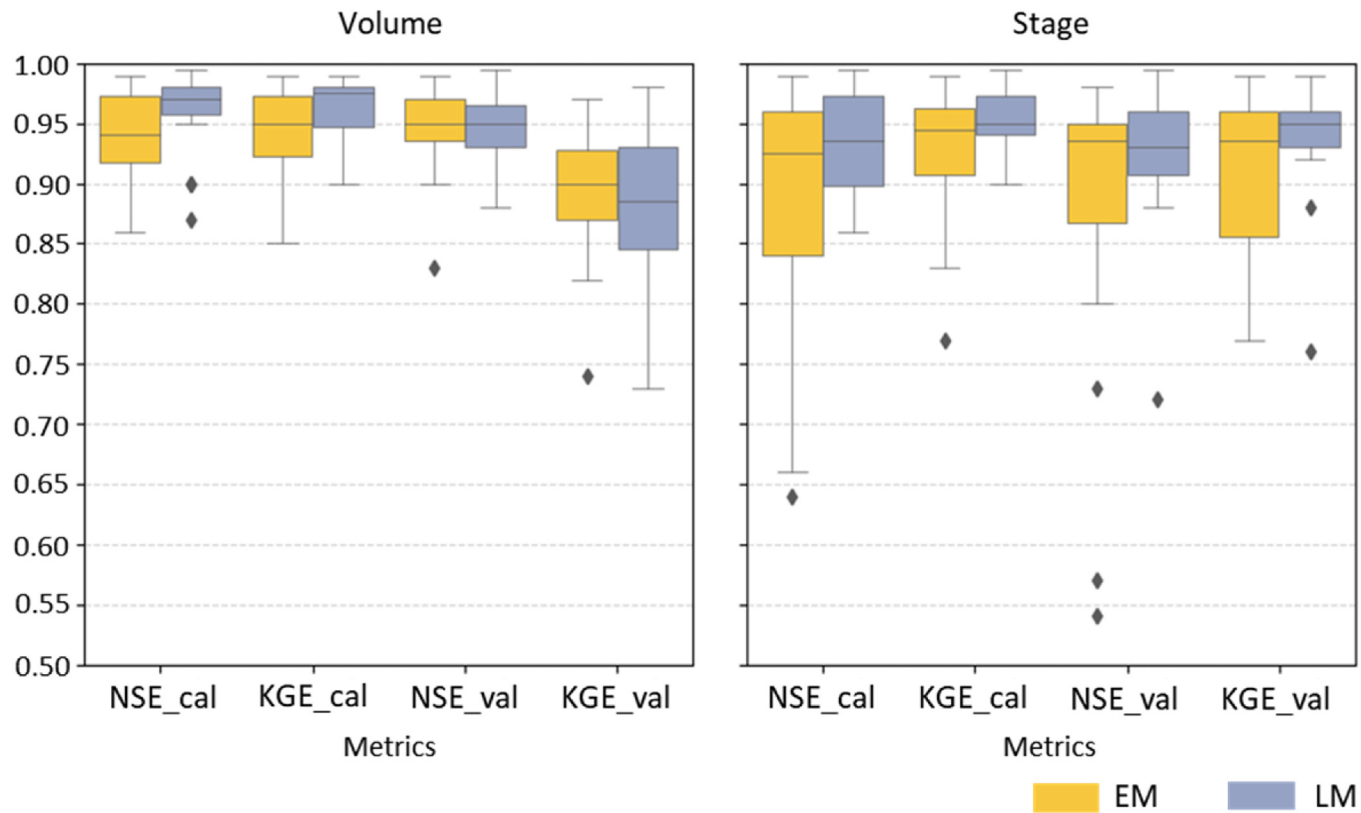
Data fit analysis based on volume and stage time series both demonstrated the potential of UISCEmod for modelling water levels in ephemeral karstic wetlands (Fig. 7). Focusing on the volume time series, NSE and KGE were above 0.85 for most of the sites for calibration and

Table 4

NSE, KGE and BIAS of the EM and LM modelling approaches at modelling volume time series. EM: Experimental model, LM:Lump model, Cal:calibration, Val:validation, IQR:Interquartile range.

Site Name	ID	EM			LM			Cal			Val		
		Cal			Val			Cal			Val		
		NSE	KGE	BIAS									
Ballycar Lough	1	0.99	0.97	0.7	0.97	0.95	1.4	0.99	0.99	0.1	0.99	0.98	-1.1
Ballygalda Turlough	2	0.98	0.95	1.5	0.98	0.90	1.8	0.98	0.99	0.1	0.98	0.93	-1.1
Blackrock	3	0.87	0.85	2.2	0.83	0.74	10.1	0.96	0.97	0.3	0.93	0.88	5.7
Caherglassaun	4	0.94	0.96	0.9	0.94	0.89	5.6	0.95	0.97	0.4	0.98	0.95	4.2
Castleplunket	5	0.91	0.94	0.7	0.92	0.90	3.4	0.97	0.98	0.3	0.94	0.74	7.7
Coole Lough	6	0.94	0.96	0.5	0.95	0.84	4.8	0.97	0.98	0.5	0.95	0.87	5.0
Fortwilliam Turlough	7	0.93	0.9	1.2	0.96	0.92	1.1	0.96	0.95	2.1	0.95	0.87	6.7
Lisduff	8	0.87	0.9	0.0	0.99	0.97	-2.7	0.9	0.93	-0.5	0.96	0.95	0.3
Lough Aleenaun	9	0.92	0.94	-0.1	0.95	0.88	1.6	0.9	0.93	-0.1	0.94	0.89	1.8
Lough Funshinagh	10	0.98	0.99	-0.4	0.9	0.83	-4.0	0.99	0.98	-0.4	0.88	0.73	-6.7
Lough Gealain	11	0.97	0.99	0.7	0.97	0.9	5.3	0.98	0.98	-0.1	0.98	0.93	2.5
Moylan Lough	12	0.98	0.93	-2.4	0.95	0.9	-1.7	0.98	0.94	-2.6	0.89	0.8	-4.6
Shrule Turlough	13	0.92	0.95	0.3	0.94	0.95	3.3	0.96	0.97	-0.3	0.95	0.85	6.6
Skealoghan	14	0.96	0.98	0.9	0.91	0.82	6.4	0.97	0.98	0.2	0.90	0.86	4.2
Termon South	15	0.97	0.98	0.3	0.98	0.97	-6.5	0.98	0.98	-0.1	0.95	0.91	-6.4
Tulla Turlough	16	0.86	0.90	0.5	0.94	0.92	-0.7	0.87	0.90	-0.1	0.93	0.90	-2.6
Mean		0.94	0.94	0.4	0.94	0.89	1.8	0.96	0.96	0.0	0.95	0.88	1.5
Median		0.94	0.95	0.6	0.95	0.90	1.7	0.97	0.98	0.0	0.95	0.89	2.1
IQR		0.06	0.05	0.7	0.04	0.06	5.9	0.02	0.03	0.5	0.04	0.09	6.6

a) Data Fit – NSE and KGE



b) Data Fit – BIAS

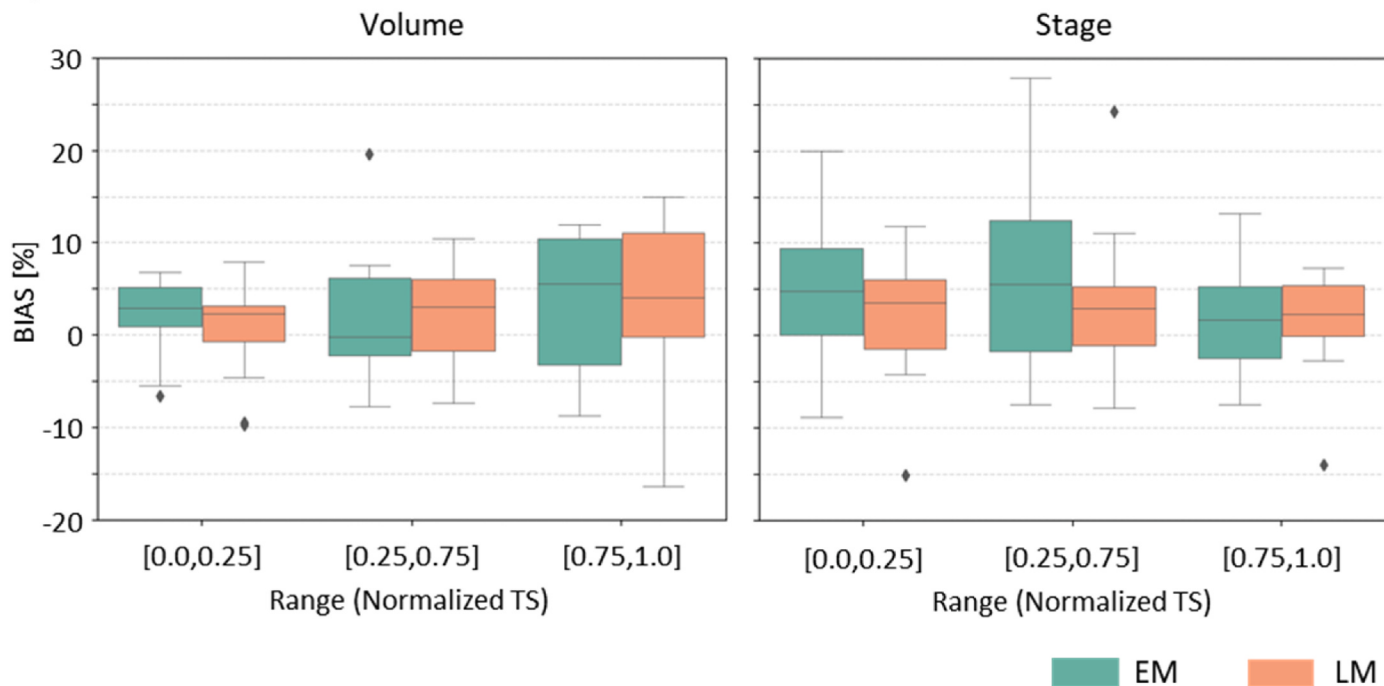


Fig. 7. Summary evaluating the capacity of the modelling approaches at constraining measured water levels in wetlands. a) Box plot showing fit of the data for both modelling approaches looking at NSE and KGE values for calibration and validation datasets. b) Box plot showing BIAS at modelling the validation datasets for volume and stage time series for different levels of floods.

a) Data Fit – Time Series

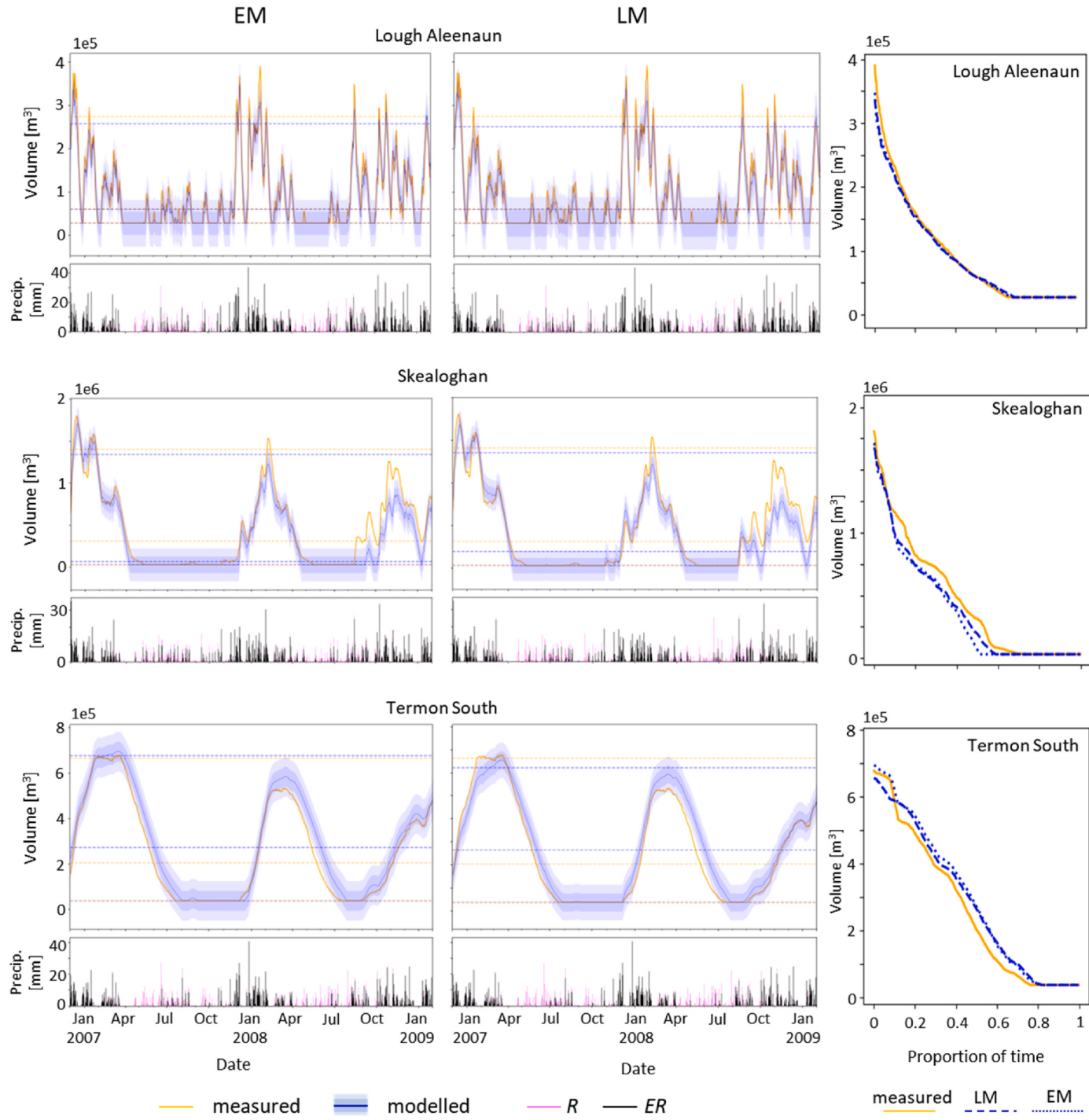


Fig. 8. a) Comparison between measured (yellow) and modelled (blue) time series used for validation. Left: EM modelling approach, Right: LM modelling approach. The horizontal dashed lines for EM and LM columns indicates the 5, 50 and 95 percentiles for modelled (blue) and measured (yellow) time series. The bar plots show rain (violet) and effective rainfall (black) associated to each site. b) Comparison of flood duration curves between measured and modelled (median) time series for the validation dataset.

validation datasets and above 0.7 for all sites. In relation to BIAS, values were between -2% and 5% for most of the sites and between -7% and 10% for all the sites (Table 4). In general, despite being small, BIAS showed a tendency towards positive values indicating a tendency to slightly underestimate the measured time series, with the largest BIAS being observed for large flood events (Fig. 7b). If we focus on the performance metrics for the calibration datasets the LM approach seems to

have a higher potential than the EM approach. However, both modelling approaches perform similarly for the validation dataset. There are two elements that may help to explain this behaviour. First, the LM approach needs to calibrate 7 model parameters versus 5 for the EM approach. Second, the current state of the LM approach, volume at time t , is dependent on the previous state, volume at time $t-1$, which makes it dependent on the initial volume conditions. This is not the case for the

TF approach, where the volume at time t is only dependent on the weighted ER from the previous days. These two characteristics means that the EM, although having less potential than the LM approach, is less likely to be overparametrized or affected by the initial conditions and may be recommended when the calibration datasets are small. In many cases model results were sufficiently accurate and equifinal, in which case the choice of model may depend on the applications.

Looking at the performance metrics for stage time series, the differences with respect to the volume time series were only due to the impact of the topography. At low water levels, small changes in volume can be related to large changes in stage, but for large floods a significant increase in volume is likely to be required to increase stage values. This means that the performance metrics for stage time series are slightly shifted towards small floods with respect to the performance metrics for the volume time series. Looking at NSE and KGE values for stage time series (Fig. 7a), the LM approach slightly outperform the EM approach for calibration and validation datasets, which would be an indicator that the LM approach is likely to be more accurate than the EM approach when modelling the floods at their lower levels. In relation to BIAS, similar values were observed for all stages of the flood, with now the largest floods having the smallest BIAS (Fig. 7b).

Finally, in addition to considering NSE, KGE and BIAS, the evaluation of the results can be complemented by comparing the distribution of the error residuals with a normal distribution based on the constrained σ parameter. Large discrepancies may indicate issues with the initial assumptions. Ignoring the segments of the data that disagree with the initial assumptions could increase confidence in the model time series and the constrained model parameters. For example, when studying large and extreme flood events, if the error residuals follow a non-normal distribution and the model has difficulty at fitting low volumes of water, it would be advised to ignore the small floods when calibrating the hydrological models.

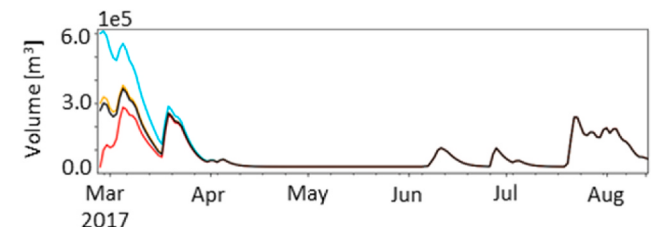
5.1.2. LM initial conditions

The LM approach requires information about the initial volume from which to start the modelling. The potential impact of spin-up period, the time it takes for the model to adjust to effects of the initial conditions, was evaluated at three representative sites (Fig. 9) considering a wide range of initial volumes: 1) measured (in black), when available, 2) high, related to observed high volumes at the site (in blue), 3) low, assuming that the site was dry (in red), and 4) medium, in between high and low (in yellow). For all but one site a single year was enough (i.e. Fig. 9a and b), but for Lough Funshinagh (ID:10) the spin up period was extended up to 6 years (Fig. 9c). In general, the spin-up period seems to be related to the k parameter of the EM approach, linked to the concept of time constant, with large k values being related to longer spin-up periods. If the initial volume is unknown but we are certain that the wetland dries every year or reaches a low stable water level, resetting point, adding an extra year at the beginning of the period to model should remove the dependency with the initial volume. If not, it may be necessary to add additional years, which has also been suggested by other works modelling water levels time series using lump-based approach (i.e. [Roo de et al. \(2013\)](#)). Finally, it is worth noticing that the analysis presented in Fig. 9 was performed with a wide range of variations of the initial conditions. The use of seasonal representative volumes of water for the specific site or the use of external information, such as local knowledge or water level estimations from satellite imagery (i.e. [McCormack et al., 2020](#)), can be considered to estimate the initial volume and shorten the spin-up period.

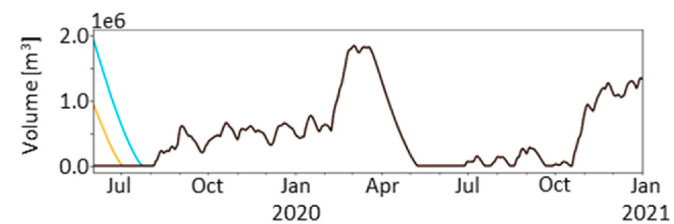
5.2. Characterization of hydrological systems

UISCEmod can also be considered as hydrological analysis tool by examining the *pdf* of the model parameters, potentially to be considered as a preliminary investigative tool prior to using and calibrating more complex hydrological models.

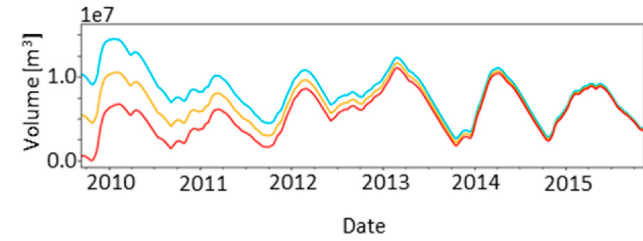
a) Lough Aleenaun



b) Skealoghan



c) Lough Funshinagh



Initial volume curve

Measured	High	Medium	Low
----------	------	--------	-----

Fig. 9. Dependency of the modelled time series on the initial volume for the LM approach for three representative sites.

The model parameters of the EM approach, despite not being directly related to the physical properties of the wetlands, can contribute to the understanding of the hydrological systems and their behaviour. Looking at each parameter individually, the constant parameter C_0^{TF} has units of volume and can be related to a potential storage capacity, volume beneath the surface of the wetland (when negative values) or to a volume of permanent water in the surface of the wetland (when positive values). The slope parameter C_1^{TF} has units of area and it is used to compute the total volume within the wetland from the weighted ER time series, including the impact of both inflow and outflow from the wetland. This means that it is not directly related to the catchment area and instead should only be considered as a scaling factor. The shape parameter, n , can be considered as a proxy for complexity of the hydrological system with large n values being related to wetlands that are more likely to have interconnections with nearby hydrological systems. Finally, the scale parameter, k , is related to the falling limbs after ceasing of wetland recharge during the recession phase. Large k values are associated to a small outflows and small k values to a large outflows from the wetland, relative to the inflow.

The combination of k and n parameters can offer additional information about the wetlands. First, they can be used to compute the mode of the gamma distribution (eq. (17)), constraining the temporal delay for the largest volume to occur after a rain event (td_{max}). This variable marks the inflection point from which inflow into the wetland from a rain event goes from being larger to smaller than the associated outflow. Second, the value of the gamma distribution associated to td_{max} , which is the proportion of ER incorporated at td_{max} , can be used as proxy to characterize the flashiness of the wetland ($f_{td_{max}}$), as large values will be

associated with flashy wetlands, while small values will be related to wetlands with smooth water levels time series.

$$td_{max} = (n - 1) \bullet k \quad \text{eq. 17}$$

Finally, by considering the length of the gamma function, td_{len} , one can get an estimation of the time that is needed for the recharge associated to a rain event to go through the hydrological system.

It is worth noticing that n , k , td_{max} , td_{len} , and $f_t td_{max}$ are independent with respect to the volumes of water within the system, and thus can be useful when evaluating behavioural patterns between wetlands.

For the LM modelling approach, the parameters related to the outflow, Qo^0, Qo^1, H_0, β , are associated with the physical properties of a simplified hydrological system where Qo^0 is a constant flow, Qo^1 is the coefficient for the variable outflow, β is the orifice coefficient for wetland discharge, and H_0 represents the elevation of the underground outflow.

Looking at the parameters related to inflow, C_1^{LM} can be considered as a notional contributing area, defining a representative zone of contribution required to generate the inflow time series within the wetland, and so can be interpreted as an effective catchment area. This estimate, however, is likely to be a lower bound and that the real catchment area can be much larger, which needs to be considered if C_1^{LM} want to be used for additional applications, such as modelling water quality. In relation to the input parameters used to constrain the inflow, the gamma function for the LM approach is applied to weight the ER that needs to be considered to change volume from V_{t-1} to V_t , instead of what happens with the EM approach where it accounts for the ER that needs to be considered to calculate the total volume at V_t . These means that gamma functions for the LM modelling approach is related to the delay for ER to be incorporated into the reservoir and needs to contemplate a smaller number of antecedent days than in the EM approach. Finally, it is worth noting that the LM approach also provides inflow and outflow time series of the wetland, which are not available from the EM approach.

5.3. Applications

UISCEmod is a data-based hydrological software that requires of minimal input information for modelling water level time series in ephemeral karstic wetlands that incorporates an automated approach for the calibration process. This makes it interesting for large-scale studies, where the hydrological properties of a large portion of the sites may not be a priori well constrained. In general, meteorological and DTM data can be accessed from national services or satellite data, but water level time series in groundwater dependent wetlands are harder to obtain due to their wide distribution. New methodological approaches for monitoring wetlands using Sentinel-1 SAR satellite images (i.e. McCormack et al., 2020 and McCormack et al., 2022)), can facilitate access to water level time series in wetlands providing continuous data since 2015. Easy access to these datasets would facilitate the use of UISCEmod to national-scale applications with potential for hindcasting, forecasting, quantification of ecohydrological variables, and assessing the impact of climate change, which could provide evidence based to inform relevant national policymakers, planners, stakeholders and researchers of potential flooding, ecological, and climate-related issues and enable the development of pre-emptive mitigation strategies.

In relation to the application to UISCEmod to new areas, it is worth remembering that the current version is relatively simple and that although it has been demonstrated to be suitable for ephemeral karstic wetlands in Ireland it will likely need some updates if applied to new environments. Because UISCEmod is based on reservoir models and build with independent modules, adaptation to new cases of study may be relatively easy. In terms of ER, applying UISCEmod to an environment where run-off plays the relevant role, instead of infiltration, the calculation of ER presented by Jakeman et al. (1990), suitable for humid region, and by Ye et al. (1998), suitable for arid regions, could be easily

incorporated into UISCEmod. In addition, potential ER time series from external sources can be added without modifying the source code, as the potential ER are calculated prior to starting the calibration process. This facilitate the use of ER time series from complex models that could be harder to implement into UISCEmod.

In terms of increasing the complexity of the hydrological models, several options can be investigated depending on the case of study. If specific characteristics of the site are known, such as additional outflows at different elevations, the LM approach can be updated to incorporate such characteristics. The use of more generalized transfer functions (i.e Beven, 2012; Taylor et al., 2007) can also be incorporated although a trans-dimensional Bayesian approach may then be required to automatically decide the number of needed reservoirs and how to connect them (series or parallel). For simpler alternative infiltration models, if we want to consider the influence of elements of the hydrological system contributing to the inflow of the wetland, such as fast and slow systems (i.e. Jakeman et al., 1990), it would be relatively easy to implement it without the need of major disruptions to the current source code, for example by modifying eq. (3) with eq. (18) for the EM approach, and eq. (5) with eq. (19) for the LM approach,

$$V = C_0^{EM} + C_1^{EM}(\alpha(f_1(t) * ER) + (1 - \alpha)(f_2(t) * ER)) \quad \text{eq. 18}$$

$$Q_t = (C_1^{LM} - A) \bullet (\alpha(f_1(t) * ER) + (1 - \alpha)(f_2(t) * ER)) \quad \text{eq. 19}$$

where α ranges between 0 and 1 and it is used to distribute the ER between the two parallel hydrological systems, and f_1 and f_2 are independent gamma distributions associated to each of the two parallel systems (i.e. fast and slow). An equivalent approach may also be considered to incorporate additional input data such as river stage, sea level, snow melt or abstractions, with the potential of having to: 1) replace ER by alternative data, 2) add additional scale factors, and 3) consider alternatives to the gamma function. However, it is worth remembering that adding more complexity to the model is also likely to increase the risk of overparameterization and to complicate the calibration process. Therefore, potential updates should be considered when requested by the specific case of study, and their advantages assessed by comparing model performance of the updated version with the current version of UISCEmod.

Finally, UISCEmod may also be considered for modelling other hydrological systems. For example, it can be used for modelling water levels in boreholes, as it is done with other codes based on gamma function (i.e. PASTAS, Collenteur et al., 2019). In this case, the main difference with the current version of UISCEmod would be the impediment for using volume stage curves for converting from volume to stage time series, and vice-versa. Although an “equivalent” volume stage curve could be estimated from the calibration process, and initial and simple approach would be to consider a 1:1 relationship between volume and stage. Another potential application would be to use USICEmod to directly model outflows, instead of water levels, which would be relatively easy to incorporate by ignoring the conversion from volume to stage and replace the output time series from volume to outflow. Despite these potential applications are technically feasible, further investigation would be required to adequately assess the potential of UISCEmod and to understand the meaning of the model parameters in these scenarios.

6. Conclusions

This manuscript presents UISCEmod, an open-source software for modelling water level time series in ephemeral karstic wetlands with an automated process for calibrating the model parameters following a Bayesian approach. UISCEmod contains both experimental, EM, and lump conceptual, LM, hydrological models and is implemented by modules and functions to facilitate future updates and facilitate their use in new areas and scenarios. The evaluation process presented in this

manuscript proves the potential of UISCEmod for modelling water level time series in ephemeral karstic wetlands with NSE and KGE values between 0.85 and 0.99 and BIAS between -2% and 5% for calibration and validation datasets for most of the evaluated sites. Estimated confidence intervals of the model time series were also validated, showing discrepancies smaller than 10% for the EM and smaller than 15% for the LM approaches for most of the sites.

In addition to modelling water level time series, UISCEmod can also be considered to characterize hydrological systems by analysing the *pdf* of the model parameters, potentially being used as a preliminary investigative tool before applying more complex hydrological models. The EM approach can be considered to quantify wetlands that are more likely to have interconnections with the surrounding hydrological systems, wetlands that react faster to rain events, wetlands with a flashy behaviour, wetlands where the floods are likely to take longer to vanish, and to estimate the residence time of water within the wetland. On the other hand, the LM approach provides relevant information such as inflow and outflow time series of the wetland, an estimate of the effective catchment area, and information about properties of the outflow and their dependency with the depth of the flood.

In terms of applications, UISCEmod can provide science based and user specific hydrological information of ephemeral karstic wetlands related to past, present and potential future climates, and has wide-ranging applications including elucidating relationship between wetland biodiversity and hydrology, flood risk management, and assessing the potential impact of climate change on critical wetland habitats.

Declaration statement

The authors declare that they have no known competing financial interests or personal relationships that could have appeared to influence the work reported in this paper.

CRediT authorship contribution statement

Joan Campanyà: Conceptualization, Methodology, Software, Validation, Formal analysis, Investigation, Data curation, Visualization, Writing – original draft, Writing – review & editing, Funding acquisition. **Ted McCormack:** Conceptualization, Formal analysis, Data curation, Writing – review & editing. **Laurence William Gill:** Methodology, Writing – review & editing. **Paul Meredith Johnston:** Methodology, Writing – review & editing. **Andrea Licciardi:** Methodology, Writing – review & editing. **Owen Naughton:** Conceptualization, Methodology, Formal analysis, Investigation, Data curation, Writing – original draft, Writing – review & editing, Supervision, Project administration, Funding Acquisition.

Software and data availability

- Data Availability:
 - Groundwater levels: Geological Survey Ireland, gwlevel.ie;
 - Meteorological data: Met Éireann, www.met.ie
- Software: UISCEmod will be available at <https://github.com/joancaampanya/UISCEmod.git>

Declaration of competing interest

The authors declare that they have no known competing financial interests or personal relationships that could have appeared to influence the work reported in this paper.

Data availability

Data will be made available on request.

Acknowledgements

This work was supported by Geological Survey Ireland [grant number: 2019-TRP-GW-001]. Data and expertise were provided by Geological Survey Ireland Groundwater and Geothermal Unit. The authors would like to thank Met Éireann for provision of meteorological data and National Parks and Wildlife Service (NPWS) for funding of acquisition of water level data in turloughs between 2006 and 2009.

We would like to thank the two anonymous reviewers for taking the time and spending the effort to provide very concise and critical remarks, which helped to significantly improve the manuscript.

References

- Allen, C., Gonzales, R., Parrott, L., 2020. Modelling the contribution of ephemeral wetlands to landscape connectivity. *Ecol. Model.* 419, 108944. <https://doi.org/10.1016/j.ecolmodel.2020.108944>.
- Ascott, M.J., Marchant, B.P., Macdonald, D., McKenzie, A.A., Bloomfield, J.P., 2017. Improved understanding of spatio-temporal controls on regional scale groundwater flooding using hydrograph analysis and impulse response functions. *Hydrol. Process.* 31, 4586–4599. <https://doi.org/10.1002/hyp.11380>.
- Basu, B., Morrissey, P., Gill, L.W., 2022. Application of nonlinear time series and machine learning algorithms for forecasting groundwater flooding in a lowland karst area. *Water Resour. Res.* 58, e2021WR029576. <https://doi.org/10.1029/2021WR029576>.
- Beaudeau, P., Leboulanger, T., Lacroix, M., Hanneton, S., Wang, H.Q., 2001. Forecasting of turbid floods in a coastal, chalk karstic drain using an artificial neural network. *Groundwater* 39, 109–118. <https://doi.org/10.1111/j.1745-6584.2001.tb00356.x>.
- Beven, K.J., 2012. *Rainfall-Runoff Modelling: the Primer, second ed.* Wiley-Blackwell.
- Bhatnagar, S., Gill, L.W., Waldren, S., Sharkey, N., Naughton, O., Johnston, P., Coxon, C., Morrissey, P., Ghosh, B., 2021. Ecohydrological metrics for vegetation communities in turloughs (ephemeral karstic wetlands). *Ecohydrology* 14, e2316. <https://doi.org/10.1002/eco.2316>.
- Bonacci, O., 2013. 6.11 poljes, ponors and their catchments. In: Shroder, J.F. (Ed.), *Treatise on Geomorphology*. Academic Press, San Diego, pp. 112–120. <https://doi.org/10.1016/B978-0-12-374739-6.00103-2>.
- Borghi, A., Renard, P., Cornaton, F., 2016. Can one identify karst conduit networks geometry and properties from hydraulic and tracer test data? *Adv. Water Resour.* 90, 99–115. <https://doi.org/10.1016/j.advwatres.2016.02.009>.
- Calhoun, A.J.K., Mushet, D.M., Bell, K.P., Boix, D., Fitzsimons, J.A., Isselin-Nondedeu, F., 2017. Temporary wetlands: challenges and solutions to conserving a ‘disappearing’ ecosystem. *Biol. Conserv.*, Small Natural Features 211, 3–11. <https://doi.org/10.1016/j.biocon.2016.11.024>.
- Casanova, M.T., Brock, M.A., 2000. How do depth, duration and frequency of flooding influence the establishment of wetland plant communities? *Plant Ecol.* 147, 237–250. <https://doi.org/10.1023/A:1009875226637>.
- Collenteur, R.A., Balkier, M., Caljé, R., Kloep, S.A., Schaars, F., 2019. Pastas: open source software for the analysis of groundwater time series. *Groundwater* 57, 877–885. <https://doi.org/10.1111/gwat.12925>.
- Costanza, R., de Groot, R., Sutton, P., van der Ploeg, S., Anderson, S.J., Kubiszewski, I., Farber, S., Turner, R.K., 2014. Changes in the global value of ecosystem services. *Global Environ. Change* 26, 152–158. <https://doi.org/10.1016/j.gloenvcha.2014.04.002>.
- Coxon, C.E., 1987. An examination of the characteristics of turloughs, using multivariate statistical techniques. *Ir. Geogr.* 20, 24–42. <https://doi.org/10.1080/00750778070478821>.
- Cvijic, J., 1893. *Das Karstphanomen: Versuch einer morphologischen Monographie, Geographische Abhandlungen*. Holzel, Wien.
- Davidson, N.C., Fluet-Chouinard, E., Finlayson, C.M., Davidson, N.C., Fluet-Chouinard, E., Finlayson, C.M., 2018. Global extent and distribution of wetlands: trends and issues. *Mar. Freshw. Res.* 69, 620–627. <https://doi.org/10.1071/MF17019>.
- De Becker, P., Hermy, M., Butaye, J., 1999. Ecohydrological characterization of a groundwater-fed alluvial floodplain mire. *Appl. Veg. Sci.* 2, 215–228. <https://doi.org/10.2307/1478985>.
- Dreiss, S.J., 1982. Linear kernels for karst aquifers. *Water Resour. Res.* 18, 865–876. <https://doi.org/10.1029/WR018i004p00865>.
- Drew, D., 2018. *Karst of Ireland: Landscape Hydrogeology Methods*. Geological Survey Ireland.
- Duran, L., Gill, L., 2021. Modeling spring flow of an Irish karst catchment using Modflow-USG with CLN. *J. Hydrol.* 597, 125971. <https://doi.org/10.1016/j.jhydrol.2021.125971>.
- Foreman-Mackey, D., 2016. corner.py: scatterplot matrices in Python. *J. Open Source Softw.* 1, 24. <https://doi.org/10.21105/joss.00024>.
- Gelman, A., Meng, X.-L., Stern, H., 1996. Posterior predictive assessment of model fitness via realized discrepancies. *Stat. Sin.* 6, 733–760.
- Geman, S., Geman, D., 1984. Stochastic relaxation, Gibbs distributions, and the Bayesian restoration of images. *IEEE Trans. Pattern Anal. Mach. Intell. PAMI* 6, 721–741. <https://doi.org/10.1109/TPAMI.1984.4767596>.
- Gill, L.W., Naughton, O., Johnston, P.M., 2013. Modeling a network of turloughs in lowland karst. *Water Resour. Res.* 49, 3487–3503. <https://doi.org/10.1002/wrcr.20299>.

- Gill, L.W., Schuler, P., Duran, L., Morrissey, P., Johnston, P.M., 2021. An evaluation of semidistributed-pipe-network and distributed-finite-difference models to simulate karst systems. *Hydrogeol. J.* 29, 259–279. <https://doi.org/10.1007/s10040-020-02241-8>.
- Gupta, H.V., Kling, H., Yilmaz, K.K., Martinez, G.F., 2009. Decomposition of the mean squared error and NSE performance criteria: implications for improving hydrological modelling. *J. Hydrol.* 377, 80–91. <https://doi.org/10.1016/j.jhydrol.2009.08.003>.
- Gutiérrez, F., Parise, M., De Waele, J., Jourde, H., 2014. A review on natural and human-induced geohazards and impacts in karst. *Earth Sci. Rev.* 138, 61–88. <https://doi.org/10.1016/j.earscirev.2014.08.002>.
- Hartmann, A., Barberá, J.A., Lange, J., Andreo, B., Weiler, M., 2013. Progress in the hydrologic simulation of time variant recharge areas of karst systems – exemplified at a karst spring in Southern Spain. *Adv. Water Resour.* 54, 149–160. <https://doi.org/10.1016/j.advwatres.2013.01.010>.
- Hartmann, A., Goldscheider, N., Wagener, T., Lange, J., Weiler, M., 2014. Karst water resources in a changing world: review of hydrological modeling approaches. *Rev. Geophys.* 52, 218–242. <https://doi.org/10.1002/2013RG000443>.
- Hartmann, A., Lange, J., Weiler, M., Arbel, Y., Greenbaum, N., 2012. A new approach to model the spatial and temporal variability of recharge to karst aquifers. *Hydrod. Earth Syst. Sci.* 16, 2219–2231. <https://doi.org/10.5194/hess-16-2219-2012>.
- Hastings, W.K., 1970. Monte Carlo sampling methods using Markov chains and their applications. *Biometrika* 57, 97–109. <https://doi.org/10.1093/biomet/57.1.97>.
- Hogg, D.W., Foreman-Mackey, D., 2018. Data analysis recipes: using Markov chain Monte Carlo. *Astrophys. J. Suppl.* 236, 11. <https://doi.org/10.3847/1538-4365/ab76e>.
- Hu, C., Hao, Y., Yeh, T.-C.J., Pang, B., Wu, Z., 2008. Simulation of spring flows from a karst aquifer with an artificial neural network. *Hydrod. Process.* 22, 596–604. <https://doi.org/10.1002/hyp.6625>.
- IPBES, 2019. Global Assessment Report on Biodiversity and Ecosystem Services. IPBES secretariat [WWW Document]. URL <https://www.ipbes.net/node/35274>. accessed April.24.23.
- Irvine, K., Coxon, C., Gill, L., Kimberley, S., Waldren, S., 2018. Turloughs (Ireland). In: Finlayson, C.M., Milton, G.R., Prentice, R.C., Davidson, N.C. (Eds.), *The Wetland Book II: Distribution, Description, and Conservation*. Springer Netherlands, Dordrecht, pp. 1067–1077. https://doi.org/10.1007/978-94-007-4001-3_256.
- Jakeman, A.J., Littlewood, I.G., Whitehead, P.G., 1990. Computation of the instantaneous unit hydrograph and identifiable component flows with application to two small upland catchments. *J. Hydrol.* 117, 275–300. [https://doi.org/10.1016/0022-1694\(90\)90097-H](https://doi.org/10.1016/0022-1694(90)90097-H).
- Johnson, W.C., Poiani, K.A., 2016. Climate change effects on prairie pothole wetlands: findings from a twenty-five year numerical modeling Project. *Wetlands* 36, 273–285. <https://doi.org/10.1007/s13157-016-0790-3>.
- Jukić, D., Denić-Jukić, V., 2006. Nonlinear kernel functions for karst aquifers. *J. Hydrol., Measurement and Parameterization of Rainfall Microstructure* 328, 360–374. <https://doi.org/10.1016/j.jhydrol.2005.12.030>.
- Klemes, V., 1986. Operational testing of hydrological simulation models. *Hydrod. Sci. J.* 31, 13–24. <https://doi.org/10.1080/0262668609491024>.
- Kling, H., Fuchs, M., Paulin, M., 2012. Runoff conditions in the upper Danube basin under an ensemble of climate change scenarios. *J. Hydrol.* 424–425, 264–277. <https://doi.org/10.1016/j.jhydrol.2012.01.011>.
- Kurtulus, B., Razack, M., 2007. Evaluation of the ability of an artificial neural network model to simulate the input-output responses of a large karstic aquifer: the La Rochefoucauld aquifer (Charente, France). *Hydrogeol. J.* 15, 241–254. <https://doi.org/10.1007/s10040-006-0077-5>.
- Mackay, J.D., Jackson, C.R., Wang, L., 2014. A lumped conceptual model to simulate groundwater level time-series. *Environ. Model. Software* 61, 229–245. <https://doi.org/10.1016/j.envsoft.2014.06.003>.
- Malinverno, A., Briggs, V.A., 2004. Expanded uncertainty quantification in inverse problems: hierarchical Bayes and empirical Bayes. *Geophysics* 69, 1005–1016. <https://doi.org/10.1190/1.1778243>.
- Mayaud, C., Gabrovšek, F., Blatník, M., Kogovšek, B., Petrič, M., Ravbar, N., 2019. Understanding flooding in poljes: a modelling perspective. *J. Hydrol.* 575, 874–889. <https://doi.org/10.1016/j.jhydrol.2019.04.092>.
- Mazzilli, N., Guinot, V., Jourde, H., Lecoq, N., Labat, D., Arfib, B., Baudement, C., Danquigny, C., Dal Soglio, L., Bertin, D., 2019. KarstMod: a modelling platform for rainfall - discharge analysis and modelling dedicated to karst systems. *Environ. Model. Software* 122, 103927. <https://doi.org/10.1016/j.envsoft.2017.03.015>.
- McCormack, T., Campanyà, J., Naughton, O., 2022. A methodology for mapping annual flood extent using multi-temporal Sentinel-1 imagery. *Remote Sens. Environ.* 282, 113273. <https://doi.org/10.1016/j.rse.2022.113273>.
- McCormack, T., Naughton, O., Bradford, R., Campanyà, J., Morrissey, P., Gill, L., Lee, M., 2020. GWFlood Project: monitoring, modelling and mapping karst groundwater flooding in Ireland [WWW Document]. URL <https://www.gsi.ie/en-ie/publications/Pages/GWFlood-Project-Monitoring-Modelling-and-Mapping-Karst-Groundwater-Flooding-in-Ireland.aspx>. accessed 6.March.22.
- Metropolis, N., Rosenbluth, A.W., Rosenbluth, M.N., Teller, A.H., Teller, E., 1953. Equation of state calculations by fast computing machines. *J. Chem. Phys.* 21, 1087–1092. <https://doi.org/10.1063/1.1699114>.
- Millennium Ecosystem Assessment, 2005. *Ecosystems and Human Well-Being: Synthesis*. Island Press, Washington, DC.
- Mitsch, W.J., Bernal, B., Hernandez, M.E., 2015. Ecosystem services of wetlands. *Int. J. Biophys. Sci. Ecosyst. Serv. Manag.* 11, 1–4. <https://doi.org/10.1080/21513732.2015.1006250>.
- Mittermeier, R.A., Turner, W.R., Larsen, F.W., Brooks, T.M., Gascon, C., 2011. Global biodiversity conservation: the critical role of hotspots. In: Zachos, F.E., Habel, J.C. (Eds.), *Biodiversity Hotspots: Distribution and Protection of Conservation Priority Areas*. Springer, Berlin, Heidelberg, pp. 3–22. https://doi.org/10.1007/978-3-642-20992-5_1.
- Morrissey, P., McCormack, T., Naughton, O., Meredith Johnston, P., William Gill, L., 2020. Modelling groundwater flooding in a lowland karst catchment. *J. Hydrol.* 580, 124361. <https://doi.org/10.1016/j.jhydrol.2019.124361>.
- Mudarra, M., Hartmann, A., Andreo, B., 2019. Combining experimental methods and modeling to quantify the complex recharge behavior of karst aquifers. *Water Resour. Res.* 55, 1384–1404. <https://doi.org/10.1029/2017WR021819>.
- Nash, J.E., 1959. Systematic determination of unit hydrograph parameters. *J. Geophys. Res.* 64, 111–115.
- Nash, J.E., 1960. A unit hydrograph study, with particular reference to british catchments. *Proc. Inst. Civ. Eng.* 17, 249–282. <https://doi.org/10.1680/iicep.1960.11649>.
- Nash, J.E., Sutcliffe, J.V., 1970. River flow forecasting through conceptual models part I — a discussion of principles. *J. Hydrol.* 10, 282–290. [https://doi.org/10.1016/0022-1694\(70\)90255-6](https://doi.org/10.1016/0022-1694(70)90255-6).
- Naughton, O., 2011. *The Hydrology and Hydroecology of Turloughs (Trinity College Dublin)*.
- Naughton, O., Johnston, P.M., McCormack, T., Gill, L.w., 2017. Groundwater flood risk mapping and management: examples from a lowland karst catchment in Ireland. *J. Flood Risk Manag* 10, 53–64. <https://doi.org/10.1111/jfr3.12145>.
- Naughton, O., Johnston, P.M., Gill, L.W., 2012. Groundwater flooding in Irish karst: the hydrological characterisation of ephemeral lakes (turloughs). *J. Hydrol.* 470–471, 82–97. <https://doi.org/10.1016/j.jhydrol.2012.08.012>.
- Naughton, O., McCormack, T., Drew, D., Gill, L., Johnston, P., Morrissey, P., Regan, S., 2018. The hydrogeology of the gort lowlands. *Ir. J. Earth Sci.* 36, 25–44. <https://doi.org/10.3318/ijes.2018.36.25>.
- NPWS, 2019. The Status of EU Protected Habitats and Species in Ireland. Volume 1: Summary Overview. Unpublished NPWS report. Link: npws.ie/sites/default/files/publications/pdf/NPWS_2019_Vol1_Summary_Article17.pdf.
- Roo de, A., Knijff van der, J., Burek, P., 2013. LISFLOOD, Distributed Water Balance and Flood Simulation Model: Revised User Manual 2013. Publications Office of the European Union, LU.
- Schuler, P., Duran, L., Johnston, P., Gill, L., 2020. Quantifying and numerically representing recharge and flow components in a karstified carbonate aquifer. *Water Resour. Res.* 56, e2020WR027717. <https://doi.org/10.1029/2020WR027717>.
- Schulte, R.P., Diamond, J., Finkele, K., Holden, N.M., Brereton, A.J., 2005. *Predicting the Soil Moisture Conditions of Irish Grasslands*.
- Seabloom, E.W., van der Valk, A.G., 2003. Plant diversity, composition, and invasion of restored and natural prairie pothole wetlands: implications for restoration. *Wetlands* 23, 1–12. [https://doi.org/10.1672/0277-5212\(2003\)023\[0001:PDCAIJ\]2.0.CO;2](https://doi.org/10.1672/0277-5212(2003)023[0001:PDCAIJ]2.0.CO;2).
- Shaw, E., 1994. *Hydrology in Practice*, third ed. Chapman & Hall, London.
- Sheehy Skeffington, M., Moran, J., O Connor, Á., Regan, E., Coxon, C.E., Scott, N.E., Gormally, M., 2006. Turloughs – Ireland's unique wetland habitat. *Biol. Conserv.* 133, 265–290. <https://doi.org/10.1016/j.biocon.2006.06.019>.
- Shin, Y.-J., Midgley, G.F., Archer, E.R.M., Arneth, A., Barnes, D.K.A., Chan, L., Hashimoto, S., Hoegh-Guldberg, O., Insarov, G., Leadley, P., Levin, L.A., Ngo, H.T., Pandit, R., Pires, A.P.F., Pörtner, H.-O., Rogers, A.D., Scholes, R.J., Settele, J., Smith, P., 2022. Actions to halve biodiversity loss generally benefit the climate. *Global Change Biol.* 28, 2846–2874. <https://doi.org/10.1111/gcb.16109>.
- Taylor, C.J., Pedregal, D.J., Young, P.C., Tych, W., 2007. Environmental time series analysis and forecasting with the Captain toolbox. *Environ. Model. Software* 22, 797–814. <https://doi.org/10.1016/j.envsoft.2006.03.002>.
- TEEB, 2010. *The Economics of Ecosystems and Biodiversity Ecological and Economic Foundations*. Earthscan, London and Washington.
- Vörösmarty, C.J., McIntyre, P.B., Gessner, M.O., Dudgeon, D., Prusevich, A., Green, P., Glidden, S., Bunn, S.E., Sullivan, C.A., Liermann, C.R., Davies, P.M., 2010. Global threats to human water security and river biodiversity. *Nature* 467, 555–561. <https://doi.org/10.1038/nature09440>.
- Waldren, S., 2015. *Turlough Hydrology, Ecology and Conservation. National Parks & Wildlife Services. Department of Arts, Heritage and the Gaeltacht, Ireland*.
- Ye, W., Jakeman, A.J., Young, P.C., 1998. Identification of improved rainfall-runoff models for an ephemeral low-yielding Australian catchment. *Environ. Model. Software* 13, 59–74. [https://doi.org/10.1016/S1364-8152\(98\)00004-8](https://doi.org/10.1016/S1364-8152(98)00004-8).
- Zacharias, I., Zamparas, M., 2010. Mediterranean temporary ponds. A disappearing ecosystem. *Biodivers. Conserv.* 19, 3827–3834. <https://doi.org/10.1007/s10531-010-9933-7>.
- Zedler, J.B., Kercher, S., 2005. Wetland resources: status, trends, ecosystem services, and restorability. *Annu. Rev. Environ. Resour.* 30, 39–74. <https://doi.org/10.1146/annurev.energy.30.050504.144248>.
- Zedler, P.H., 2003. Vernal pools and the concept of “isolated wetlands.”. *Wetlands* 23, 597–607. [https://doi.org/10.1672/0277-5212\(2003\)023\[0597:VPATCO\]2.0.CO;2](https://doi.org/10.1672/0277-5212(2003)023[0597:VPATCO]2.0.CO;2).